Neuroscience 147 (2007) 207–223

SELECTIVE ANTEROGRADE TRACING OF THE INDIVIDUAL SEROTONERGIC AND NONSEROTONERGIC COMPONENTS OF THE DORSAL RAPHE NUCLEUS PROJECTION TO THE VESTIBULAR NUCLEI

A. L. HALBERSTADT[a] AND C. D. BALABAN[a,b]*

[a]*Department of Otolaryngology, Eye and Ear Institute, Room 107, 203 Lothrop Street, University of Pittsburgh, Pittsburgh, PA 15213, USA*

[b]*Departments of Neurobiology, Communication Sciences & Disorders, and Bioengineering, University of Pittsburgh, Pittsburgh, PA 15213, USA*

Abstract—It is well known that the dorsal raphe nucleus (DRN) sends serotonergic and nonserotonergic projections to target regions in the brain stem and forebrain, including the vestibular nuclei. Although retrograde tracing studies have reported consistently that there are differences in the relative innervation of different target regions by serotonergic and nonserotonergic DRN neurons, the relative termination patterns of these two projections have not been compared using anterograde tracing methods. The object of the present investigation was to trace anterogradely the individual serotonergic and nonserotonergic components of the projection from DRN to the vestibular nuclei in rats. To trace nonserotonergic DRN projections, animals were pretreated with the serotonergic neurotoxin 5,7-dihydroxytryptamine (5,7-DHT), and then, after 7 days, the anterograde tracer biotinylated dextran amine (BDA) was iontophoretically injected into the DRN. In animals treated with 5,7-DHT, nonserotonergic BDA-labeled fibers were found to descend exclusively within the ventricular plexus and to terminate predominantly within the periventricular aspect of the vestibular nuclei. Serotonergic DRN projections were traced by injecting 5,7-DHT directly into DRN, and amino–cupric–silver staining was used to visualize the resulting pattern of terminal degeneration. Eighteen hours after microinjection of 5,7-DHT into the DRN, fine-caliber degenerating serotonergic terminals were found within the region of the medial vestibular nucleus (MVN) that borders the fourth ventricle, and a mixture of fine- and heavier-caliber degenerating serotonergic terminals was located further laterally within the vestibular nuclear complex. These findings indicate that fine-caliber projections from serotonergic and nonserotonergic DRN neurons primarily innervate the periventricular regions of MVN, whereas heavier-caliber projections from serotonergic DRN neurons innervate terminal fields located in more lateral regions of the vestibular nuclei. Thus, serotonergic and nonserotonergic DRN axons target distinct but partially overlapping terminal fields within the vestibular nuclear complex, raising the possibility that these two DRN projection systems are organized in a manner that permits regionally-specialized regulation of processing within the vestibular nuclei.

Key words: vestibular nuclei, anterograde tracing, rats, dorsal raphe nucleus, locus coeruleus, 5;7-dihydroxytryptamine.

The dorsal raphe nucleus (DRN), located in the midbrain and rostral pons, is the largest 5-HT-containing nucleus in the brain. DRN cells project widely throughout the CNS, targeting most of the structures in the forebrain, midbrain, and brainstem (Vertes, 1991; Sim and Joseph, 1993; Vertes and Kocsis, 1994; Morin and Meyer-Bernstein, 1999). Serotonergic DRN neurons are clustered within dorsomedial (DRNdm), ventromedial (DRNvm), and lateral (DRNl) cell groups (Steinbusch et al., 1981). Although the DRN contains more than half of all the serotonergic neurons in the brain (Leger and Wiklund, 1982), approximately 50–75% of DRN cells are nonserotonergic (Moore, 1981). Hence, it is clear that targets of DRN innervation receive input from both serotonergic and nonserotonergic cells. Retrograde tracing studies reveal that the percentage of extrinsically-projecting DRN neurons which are 5-HT-positive varies depending upon the target region, with reported values ranging from 15% to >97% (O'Hearn and Molliver, 1984; Beitz et al., 1986; Ma et al., 1991; Petrov et al., 1992; Van Bockstaele et al., 1993; Datiche et al., 1995; Kirifides et al., 2001; Kim et al., 2004).

DRN projections are known to modulate the firing activity of neurons in the vestibular nuclei (Kishimoto et al., 1991; Licata et al., 1995), and a large amount of clinical evidence indicates that 5-HT acts to regulate vestibular processing (Johnson, 1998; Staab et al., 2002, 2004; Perna et al., 2003; Drummond, 2005; Simon et al., 2005; Staab and Ruckenstein, 2005; Marcus and Furman, 2006). In fact, the interaction between 5-HT and vestibular function may contribute to the observed linkage between vestibular dysfunction and anxiety disorders (reviewed by Balaban and Thayer, 2001; Balaban, 2002) and migraine (reviewed by Furman et al., 2005; Marcus et al., 2005). Retrograde tracing studies (Halberstadt and Balaban, 2003, 2006a) have demonstrated that the DRN sends an appreciable projection to the vestibular nuclei, with approximately equal proportions originating from serotonergic and nonserotonergic neurons. Anterograde tracing studies with biotinylated dextran amine (BDA) have shown that projections from the DRN terminate heavily within two

*Correspondence to: C. Balaban, University of Pittsburgh, Department of Otolaryngology, Eye and Ear Institute, Room 107, 203 Lothrop Street, Pittsburgh, PA 15213 USA. Tel: +1-412-647-2298; fax: +1-412-647-0108.
E-mail address: cbalaban@vms.cis.pitt.edu (C. Balaban).

Abbreviations: BDA, biotinylated dextran amine; DRN, dorsal raphe nucleus; DRNdm, dorsomedial dorsal raphe nucleus subdivision; DRNl, lateral dorsal raphe nucleus subdivision; DRNvm, ventromedial dorsal raphe nucleus subdivision; IVN, inferior vestibular nucleus; LC, locus coeruleus; LVN, lateral vestibular nucleus; mlf, medial longitudinal fasciculus; MVN, medial vestibular nucleus; PBS, phosphate-buffered saline; SERT, 5-HT transporter; SVN, superior vestibular nucleus; 5, 7-DHT, 5,7-dihydroxytryptamine.

0306-4522/07$30.00+0.00
doi:10.1016/j.neuroscience.2007.03.049

discrete regions of the vestibular nuclear complex (Halberstadt and Balaban, 2006b). The ipsilateral DRN projects to a rostrodorsal vestibular terminal field in the ventral aspect of the superior vestibular nucleus (SVN), the dorsal pole of the rostral two-thirds of the medial vestibular nucleus (MVN), and the dorsal part of the lateral vestibular nucleus (LVN). Both the ipsilateral and contralateral DRN project to a caudoventral vestibular terminal field that spans the ventral pole of mid-level MVN, all of caudal MVN, and the ventral part of caudal LVN.

Because there are differences in the firing activity and response properties of putative serotonergic and nonserotonergic DRN units (Aghajanian et al., 1978; Sakai and Crochet, 2001; Waterhouse et al., 2004), the ultimate influence of DRN afferents on processing within specific regions of the vestibular nuclei is likely to depend on the local organization and termination patterns of the individual serotonergic and nonserotonergic DRN projections. However, little is known regarding the comparative distribution of serotonergic and nonserotonergic DRN projections within individual target regions, including the vestibular nuclei. A number of studies have combined anterograde tracing with immunofluorescent staining for either 5-HT (Kosofsky and Molliver, 1987; Li et al., 2000; Thompson and Thompson, 2001; Aznar et al., 2004) or the 5-HT transporter (SERT) (Simpson et al., 2003) in order to examine the organization of serotonergic versus nonserotonergic DRN projections. Unfortunately, it appears that neither of these immunohistochemical methods can be used to distinguish reliably between the two classes of DRN projections. For example, the intensity of 5-HT immunostaining is dependent on the endogenous level of the transmitter (Datiche et al., 1995), and there is evidence that variations in axonal concentrations of 5-HT can lead to a substantial underestimation of the density of 5-HT-positive fibers (Nielsen et al., 2006). Immunofluorescent staining for SERT is also unreliable because heavy caliber serotonergic fibers do not co-localize SERT with 5-HT (Brown and Molliver, 2000; Nielsen et al., 2006). The latter finding is particularly germane to the issue of tracing serotonergic projections to the vestibular nuclei because the vestibular nuclei are innervated by heavier caliber projections from DRN (Halberstadt and Balaban, 2006b).

Selective serotonergic neurotoxins, including 5,7-dihydroxytryptamine (5,7-DHT), have been shown to disrupt axonal transport in serotonergic neurons (Moore and Halaris, 1975; Halaris et al., 1976; Azmitia and Segal, 1978; Jacobs et al., 1978; Moore et al., 1978; Satoh, 1979; Araneda et al., 1980a,b; Zhou and Azmitia, 1983; Callahan et al., 2001). Therefore, this study used BDA injections after 5,7-DHT-induced denervation of central serotonergic neurons to selectively trace the projections of nonserotonergic DRN neurons. Conversely, the distribution of degenerating serotonergic DRN terminals in the vestibular nuclei was identified using amino–cupric–silver staining (de Olmos et al., 1994) after microinjection of 5,7-DHT to produce small chemical lesions of serotonergic cell bodies in the DRN.

EXPERIMENTAL PROCEDURES

All procedures involving animals were approved by the Institutional Animal Care and Use Committee of the University of Pittsburgh, which certifies compliance with National Institutes of Health and United States Department of Agriculture standards for humane animal utilization. All efforts were made to minimize the number of animals used and their suffering. Pairs of animals were housed in suspended caging at 22 °C with a 12-h light/dark cycle and *ad libitum* access to food and water.

Tracing nonserotonergic projections from DRN to the vestibular nuclei

The animals were pretreated with 5,7-DHT to ablate central serotonergic neurons. After a 7-day period to permit degeneration, BDA was used to selectively anterogradely trace nonserotonergic DRN projections to the vestibular nuclei.

Surgical procedures. Twelve adult male Long-Evans rats (250–300 g; Charles River Laboratories, Wilmington, MA, USA) were anesthetized using a mixture of ketamine (50 mg/kg, i.m.), xylazine (6 mg/kg, i.m.), and acepromazine (0.5 mg/kg, i.m.). Thirty minutes after injection of nomifensine maleate (15 mg/kg, i.p.) and desipramine hydrochloride (15 mg/kg, i.p.) to prevent damage to dopaminergic and noradrenergic projections, respectively (Björklund et al., 1975; Baumgarten et al., 1982; Caillé et al., 2002), rats were administered 5,7-DHT creatinine sulfate (Fluka, Milwaukee, WI, USA) by the i.c.v. route. A 20 μl Hamilton syringe (Hamilton, Reno, NV, USA), containing a 150 μg 5,7-DHT dose (calculated as the free base: 1 μg free base=2.099 μg 5,7-DHT creatinine sulfate) in a vehicle of 15 μl 0.9% sterile saline containing 0.2% ascorbic acid, was introduced stereotaxically through a burr hole in the cranium that was centered 1 mm caudal and 1 mm to the left of bregma. The injection was made into the left lateral ventricle at a depth of 4 mm from the skull surface over a 15 min period. The burr hole was then closed with Gelfoam and the scalp incision sutured.

Seven days later, the animals were anesthetized (see above), and then positioned in a stereotaxic apparatus. A burr hole was drilled in the cranium, and a solution of 7.5% BDA (10,000 MW; Molecular Probes, Eugene, OR, USA) in 10 mM phosphate-buffer containing 0.5 M NaCl, pH 7.0, was injected iontophoretically (4 μA positive pulsed square wave, 15 s duty cycle, 15 min on-time) into DRN using glass micropipettes ($\sim$40 μm tip diameter). A 14-day post-5,7-DHT survival period (i.e. 7 days after BDA injection) was used because it produces a profound loss of markers for serotonergic DRN cells (Serrats et al., 2005; Hajós and Sharp, 1996; Bendotti et al., 1990).

Killing, fixation and sectioning. After a 7-day survival period, rats were killed with sodium pentobarbital (100 mg/kg, i.p.), and perfused transcardially with phosphate-buffered saline (PBS; 0.9% NaCl in 50 mM phosphate-buffer, pH 7.3) followed by paraformaldehyde–lysine–periodate fixative (10% paraformaldehyde, 75 mM L-lysine, 10 mM sodium periodate, and 40 mM sucrose in 50 mM phosphate-buffer, pH 7.4; McLean and Nakane, 1974). The brains were extracted from the skulls, cryoprotected for 48–72 h at 4°C in 30% sucrose–PBS, and 35 μm sections were cut in the transverse plane on a freezing–sliding microtome.

Tissue processing for SERT and BDA. Tissue sections were processed for either SERT-immunoreactivity or BDA labeling. A one-step avidin–biotin–peroxidase procedure was used to visualize BDA labeling, as described previously (see Halberstadt and Balaban, 2006b). Immunoreactivity for SERT was visualized using previously established procedures (see Halberstadt and Balaban, 2003). The mouse monoclonal anti-SERT antibody used to detect SERT-immunoreactivity (MAB1564; Chemicon International, Temecula, CA, USA) was prepared against a rat neuronal SERT NH_2-terminus/glutathione *S*-transferase fusion protein cor-

responding to the first 85 amino acids of rat SERT. This antiserum stains bands of 73 kD and 120 kD molecular weight on Western blot (Inazu et al., 2001). The distribution of serotonergic DRN neurons stained with this antiserum was consistent with that reported previously by studies using immunostaining for 5-HT (e.g. Steinbusch, 1981).

Tracing serotonergic projections from DRN to the vestibular nuclei

In order to map the distribution of serotonergic DRN terminals within the vestibular nuclei, 5,7-DHT was injected directly into DRN and amino–cupric–silver staining was used to visualize the resulting pattern of terminal degeneration. Because the optimal postoperative survival for demonstrating neuronal degeneration varies depending on the part of the fiber system examined (de Olmos et al., 1981; Switzer, 2000), we performed initial calibration experiments to verify that, as in earlier studies (Ricaurte et al., 1985; Commins et al., 1987a,b; Jensen et al., 1993), terminal degeneration was detected best under our experimental conditions at approximately 18 h after 5,7-DHT administration.

Surgical procedures. Twenty-three adult male Long-Evans rats (250–300 g; Charles River Laboratories) were anesthetized using a mixture of ketamine (50 mg/kg, i.m.), xylazine (6 mg/kg, i.m.), and acepromazine (0.5 mg/kg, i.m.), and then positioned in a stereotaxic apparatus. A burr hole was drilled in the cranium, and 30 min after injection of nomifensine maleate (15 mg/kg, i.p.) and desipramine hydrochloride (15 mg/kg, i.p.), 10 μg of 5,7-DHT in 0.5 μl of 0.9% sterile saline containing 0.2% ascorbic acid was injected into DRN using a 1 μl Hamilton syringe. As the vestibular nuclei are known to receive serotonergic innervation from caudal serotonergic raphe nuclei (Halberstadt and Balaban, 2003), for this experiment we chose not to administer 5,7-DHT by the i.c.v. route because interpretation of the results would have been confounded by the fact that 5,7-DHT is toxic to serotonergic neurons in the caudal raphe nuclei (Loewy, 1981).

Killing and fixation. Rats were killed with sodium pentobarbital (100 mg/kg, i.p.), perfused transcardially with rinse solution (0.4% sucrose, 0.8% NaCl, 0.4% dextrose and 0.023% $CaCl_2$ in 67 mM cacodylate buffer, pH 7.2–7.4) followed by fixative (4% paraformaldehyde and 4% sucrose in 67 mM cacodylate buffer, pH 7.2–7.4). After a 24 h period of storage at 4 °C, the brains were extracted from the skulls and cryoprotected in perfusion fixative containing 30% sucrose at 4 °C for 5–7 days.

Amino–cupric–silver staining and 5-HT immunostaining. The brains from 16 5,7-DHT-injected animals were shipped to NeuroScience Associates (Knoxville, TN, USA) for amino–cupric–silver staining, neutral red counterstaining, and 5-HT immunostaining. After being transferred to NeuroScience Associates, the 16 brains were embedded in a solid gelatin matrix (Switzer, 2000), sectioned (coronal plane) at 40 μm, and sets of every sixth section were collected. One set of sections was stained using the amino–cupric–silver technique (de Olmos et al., 1994) and then counterstained using Neutral Red. A second set of sections was immunostained for 5-HT. Briefly, after treatment with hydrogen peroxide and then with blocking serum, the sections were incubated with (1) a 1:750,000 dilution of polyclonal rabbit anti-5-HT antibody (Immunostar, Hudson, WI, USA) for 24 h at 4 °C, (2) a 1:200 dilution of goat anti-rabbit biotinylated secondary antibody (Vector Laboratories) for 30 min, and (3) Vectastain ABC reagent for 1 h, with thorough rinses between steps. Sections were then treated with 3,3′-diaminobenzidine tetrahydrochloride (DAB) chromagen. After completion of the staining procedures, the sections were mounted on gelatin/chrome alum-subbed slides, air-dried, dehydrated through a graded series of ethanol, cleared with xylene, and coverslipped with DPX Mountant (Fluka). A third set of sections was shipped back to our laboratory for Fluoro-Jade B staining. The primary antibody used for 5-HT immunostaining (Immunostar #20080) was prepared against 5-HT coupled to bovine serum albumin with paraformaldehyde; the pattern of staining obtained with this antibody is identical to that reported by previous 5-HT immunostaining studies (e.g. Steinbusch, 1981).

Fluoro-Jade B staining. Fluoro-Jade B, a fluorescent marker of neuronal degeneration (Schmued and Hopkins, 2000), was used to assess the distribution of DRN neuronal degeneration induced by local injection of 5,7-DHT. Briefly, the gelatin matrix-embedded sections were mounted on gelatin/chrome alum-subbed slides, transferred to 0.06% potassium permanganate for 10 min with agitation, washed with distilled water for 2 min, incubated for 20 min in a solution of 0.0004% Fluoro-Jade B (freshly prepared by adding 4 ml of a 0.01% stock solution of Fluoro-Jade B (Chemicon International) to 96 ml of 0.1% acetic acid), and then rinsed with distilled water (3×1 min). The slides were thoroughly dried in an oven at 40 °C, cleared with xylene, and coverslipped with DPX Mountant. Sections stained with Fluoro-Jade B were examined under fluorescent illumination, using a Nikon Eclipse E600N microscope equipped with a DAPI/FITC/Texas Red triple-band filter cube (Chroma Technology Corporation, Rockingham, VT, USA) and a 469–499 nm excitation filter (Chroma).

Analysis

Digital images were prepared using a Nikon Eclipse E600N microscope equipped with a Spot RT Monochrome camera (Model 2.1.1, Diagnostic Instruments, Inc., Sterling Heights, MI, USA). The images were captured on a Pentium-based computer running MetaMorph software (Ver. 6.1r4, Universal Imaging Corporation, Downingtown, PA, USA). Adobe Photoshop 7.01 (Adobe Systems, San Jose, CA, USA) was used for brightness and contrast adjustments and cropping.

Camera lucida drawings were prepared using an Olympus BH-2 microscope (20× objective) equipped with a drawing tube (Olympus, Tokyo, Japan). The full-size drawings were reduced by 50%, traced in India ink, and scanned at 600–800 dpi in grayscale mode.

RESULTS

BDA anterograde tracing of nonserotonergic DRN projections

Effect of 5,7-DHT on SERT immunostaining of DRN cells. The toxic effect of i.c.v. administration of 5,7-DHT on serotonergic neurons in the DRN was verified using SERT immunostaining in four of the 5,7-DHT-pretreated rats injected with BDA. Sections from normal animals (n=4) and from 5,7-DHT-pretreated animals that had received an iontophoretic injection of BDA into the DRN (n=4) were stained simultaneously for SERT-immunoreactivity. In control tissue from untreated animals, numerous SERT-positive cell bodies and fibers were found scattered throughout the DRN within the dorsomedial, ventromedial, and lateral subdivisions (Fig. 1A). However, 14 days after administration of 150 μg 5,7-DHT into the left lateral ventricle, there was a complete loss of SERT staining in the DRN (Fig. 1B). In animals treated with 5,7-DHT, SERT-immunopositive neurons were completely absent within the DRN. These findings demonstrate that i.c.v. administration of 150 μg 5,7-DHT has profound effects on SERT expression by serotonergic DRN cells.

BDA injection sites. Of the 12 animals pretreated with 150 μg 5,7-DHT i.c.v. that received iontophoretic BDA injections, 7 had injection sites that were centered in the

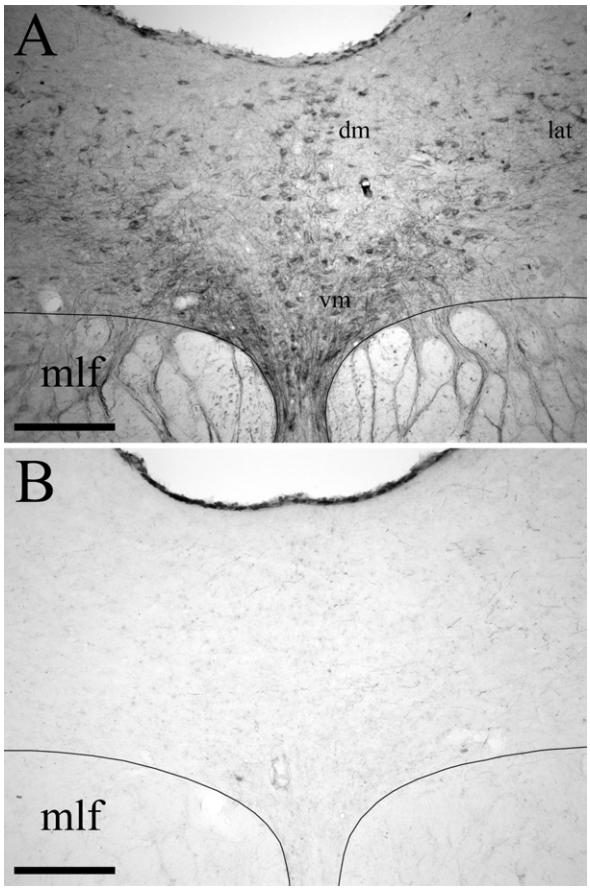

Fig. 1. Effect of i.c.v. 5,7-DHT on SERT immunostaining in the DRN. (A) In normal animals, numerous SERT-positive cell bodies, dendrites, and fibers are localized within the dorsomedial (dm), ventromedial (vm), and lateral (lat) subdivisions of DRN. (B) Fourteen days after administration of 5,7-DHT there is a marked loss of SERT immunostaining in DRN. The mlf is also indicated. Scale bars=200 μm.

DRN with minimal involvement of adjacent structures. The BDA injection sites from four of these cases are illustrated in Fig. 2. The BDA injection sites displayed a dense central core of labeled neuronal somata and neuropil surrounded by a peripheral region containing scattered neuronal perikarya with dendrites that extend into the core. These sites were generally ovoid and relatively small, with the diameter of the central core typically measuring 200 μm in the mediolateral direction and extending for a similar distance rostrocaudally across transverse sections. Injection cases DHT-214A, DHT-222B, DHT-324B and DHT-331B involved both the caudal and intermediate levels of the DRN, and injection sites DHT-222C, DHT-324A, and DHT-709A were centered within the intermediate part of DRN. The BDA injection sites were centered within different subdivisions of the DRN, although they often spanned multiple subdivisions. Injection cases DHT-222C (Fig. 2A) and DHT-324B (not shown) were relatively confined within DRNl. Case DHT-324A (not shown) was situated in DRNl with some spread into the medial longitudinal fasciculus (mlf). The injection sites in cases DHT-214A (Fig. 2B) and DHT-222B (not shown) were located in DRNl with some involvement of medial DRN subdivisions. The injection site in case DHT-331B (Fig. 2C) was primarily located within DRNdm, but also involved DRNvm and bilateral aspects of DRNl. Finally, the tracer injection in case DHT-709A (Fig. 2D) was made into DRNdm and the dorsal part of DRNvm.

Course of BDA-labeled fibers descending from DRN. Fibers descended from DRN to the vestibular nuclei within the ventricular plexus, primarily on the side ipsilateral to the injection site. Within the caudal part of DRN, fine labeled fibers coursed dorsolaterally from DRN into the periaqueductal gray, adjacent to the border of the cerebral aqueduct. As these fibers descended within the ventricular and periventricular plexus, some fibers gradually fanned out dorsally along the edge of the fourth ventricle. Within the rostral pons—especially at levels immediately caudal to the part of DRN that was designated as group B6 by Dahlström and Fuxe (1964)—a number of fine fibers exited dorsolaterally from the ventricular fiber plexus and entered the caudal third of locus coeruleus (LC), where many of them ramified heavily (Fig. 3A). A group of the fibers traversed the caudal aspect of LC; when these fibers emerged from the lateral margin of LC they turned ventrolaterally before terminating in the rostral aspect of SVN (Fig. 3B). This pattern of labeling was apparent in all injection cases, although it was especially pronounced in cases DHT-222C (see Fig. 4B) and DHT-324A. Also within the rostral pons, an extensive fiber network was located on the ventral border of the fourth ventricle (see level A of Fig. 4). At this level, a dense plexus of extremely convoluted, highly-branched, fine-caliber varicose fibers extended ventrally (and to a lesser extent ventrolaterally) from the ventricular plexus (Fig. 3C). Large numbers of fibers then traversed the posterodorsal tegmental nucleus, mlf, and to a smaller extent, nucleus subcoeruleus. Further caudally (at levels B and C of Fig. 4), this fiber network provided dense innervation to the supragenual nucleus and light innervation to the genu of the facial nucleus. This fiber network also innervated nucleus prepositus hypoglossi. This staining pattern was especially dense in cases DHT-324B, DHT-324A, and DHT-331B.

It was shown previously (Halberstadt and Balaban, 2006b) that an injection of BDA into the DRN of normal animals labels numerous heavier caliber nonvaricose fibers that descend to the vestibular nuclei within the mlf. Importantly, after treatment with 5,7-DHT, although labeled fibers could be seen traversing the mlf, no labeled fibers were observed descending from DRN within mlf (Fig. 3C, D). This finding was consistent across all 5,7-DHT-pretreated cases. The only labeled fibers that were detected within the mlf in these animals belonged to the network of fine fibers that extends ventrally from the ventricular plexus across the mlf.

Morphological appearance of labeled fibers within the vestibular nuclei. After injection of BDA into the DRN of 5,7-DHT-pretreated animals, only fine and very-fine caliber fibers were labeled anterogradely within the vestibular nuclei. Examples of labeled fibers in SVN and MVN are shown in Fig. 5A, B, respectively. These small caliber

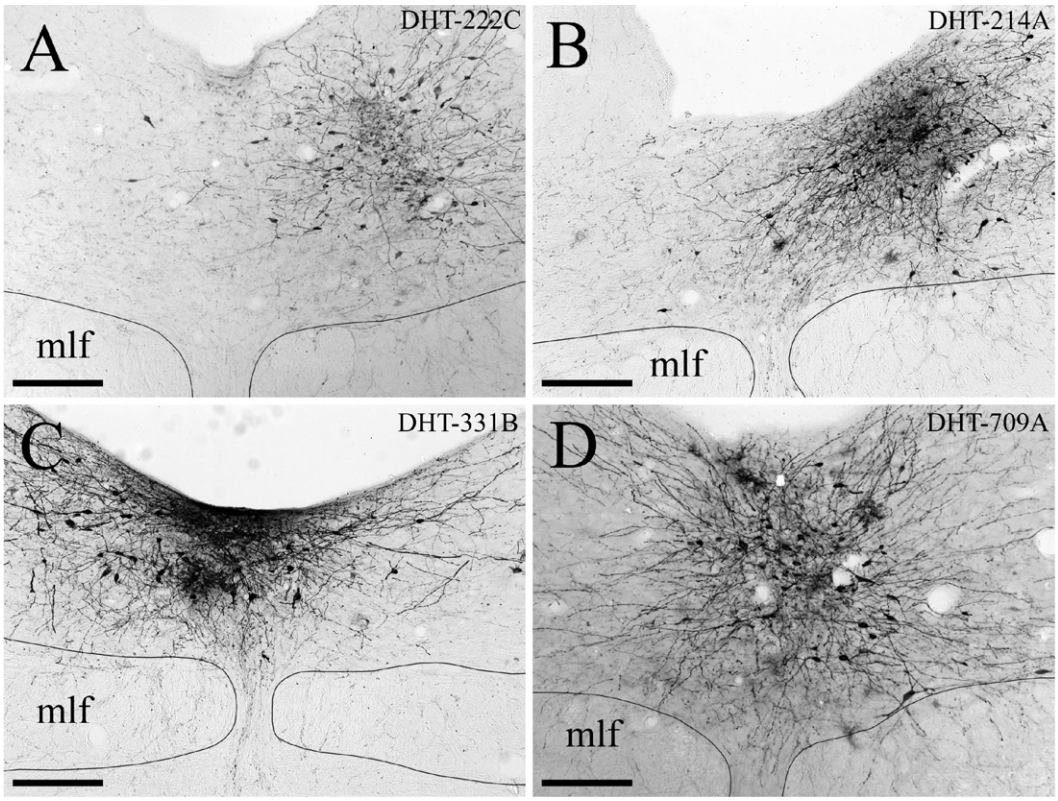

Fig. 2. Photomicrographs of the BDA injection sites in the DRN in (A) case DHT-222C, (B) case DHT-214A, (C) case DHT-331B, and (D) case DHT-709A. The mlf is also indicated. Scale bars=200 μm.

labeled fibers had pleomorphic varicosities and were identical in appearance to the small caliber fibers labeled with BDA in untreated animals (see Halberstadt and Balaban, 2006b). Although larger caliber varicose and nonvaricose fibers were labeled anterogradely from DRN in the vestibular nuclei of normal animals (Halberstadt and Balaban, 2006b), especially at sites within the vestibular nuclei that are not immediately adjacent to the fourth ventricle (see Fig. 5C), these larger labeled axons were never observed within the vestibular nuclei in animals treated with 5,7-DHT (Fig. 5D).

Distribution of labeled fibers within the vestibular nuclei. The distribution of fibers and terminal regions within the vestibular nuclei was consistent across cases. Although there was little difference in the overall pattern of labeling, the density of labeled fibers did vary between cases. However, there was no obvious relationship between the number (or density) of fibers labeled anterogradely in the vestibular nuclei and the mediolateral, dorsoventral or anteroposterior location of the injection site. The distribution of BDA-labeled fibers within five representative transverse sections spanning the rostrocaudal extent of the vestibular nuclei from case DHT-222C is illustrated in Fig. 4, respectively. Transport ipsilateral to the injection site is illustrated to the right side of the figure. The terminal innervation of the vestibular nuclei was located primarily ipsilateral to the injection site when the injection site was confined unilaterally; the projections were more symmetric in the injection cases that involved DRN bilaterally (i.e. cases DHT-331B and DHT-709A). Within the vestibular nuclei, the highest density of labeled fibers was found within the medial portions of MVN. The fibers in MVN were of fine caliber and appeared to originate from the ventricular plexus. In all injection cases, a plexus of labeled fibers was observed along the ventricular surface of MVN, and fibers from this ventricular plexus were found to extend laterally into periventricular regions of MVN (Fig. 5D).

Scattered labeled axons were also observed in the dorsolateral and ventrolateral aspects of MVN in all cases. However, as illustrated in Fig. 5D, many fewer axons were present in lateral regions of MVN than in medial MVN. This pattern of labeling is in clear contrast to that observed in normal animals (see Halberstadt and Balaban, 2006b; Fig. 5C), where BDA-labeled fibers were especially numerous in lateral MVN.

Even though the density of labeled fibers within the vestibular nuclei of animals pretreated with 5,7-DHT was greatest within MVN, labeled fibers were also observed further laterally, particularly in rostral portions of the vestibular nuclei. The ventral aspect of rostral SVN received a dense innervation (Figs. 3B and 5A), and it was also not unusual to find labeling within more caudal parts of SVN. Conversely, the fiber density in rostral LVN (level C of Fig. 3) and caudal LVN (level D of Fig. 3) was typically light, and the lowest density of fibers was present throughout the inferior vestibular nucleus (IVN).

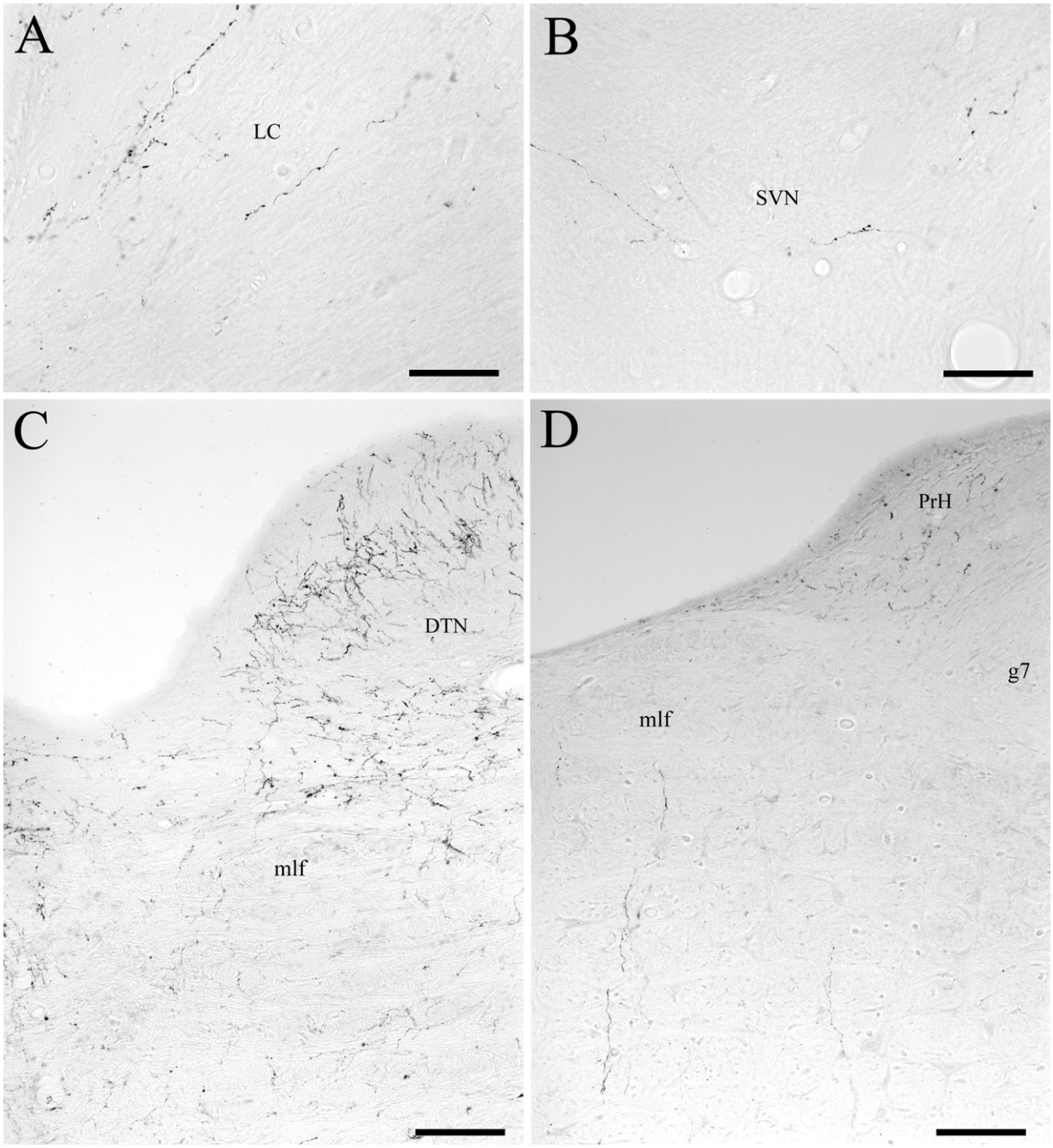

Fig. 3. Photomicrographs of anterogradely labeled fibers descending from DRN to the vestibular nuclei. (A) Within the rostral pons, fine caliber fibers coursing dorsolaterally from the ventricular fiber plexus ramify within caudal LC. Note the absence of heavier caliber fibers within LC. (B) Fine caliber fibers from the ventricular plexus also innervate rostral SVN. (C) In the rostral pons, an extensive fiber network extends ventrally and ventrolaterally from the ventricular plexus, with large numbers of fibers traversing the posterodorsal tegmental nucleus (DTN) and the mlf. Note the absence of heavier caliber fibers descending in the mlf pathway. (D) Further caudally, the density of this fiber network declines, and it provides only light innervation to the genu of the facial nucleus (g7). The location of nucleus prepositus hypoglossi (PrH) is also indicated. Scale bars=50 μm in A and B, 100 μm in C and D.

Anterograde tracing of serotonergic DRN projections

Targeting of intra-DRN 5,7-DHT injections: overview. Three criteria were used to identify the extent of a 5,7-DHT lesion within the DRN: (1) regional loss of 5-HT-immunopositive cell bodies; (2) regional distribution of silver-impregnated degenerating neuronal perikarya (see description below) in sections stained with the amino–cupric–silver technique; and (3) regional distribution of Fluoro-Jade B-positive neuronal perikarya. Cases in which the

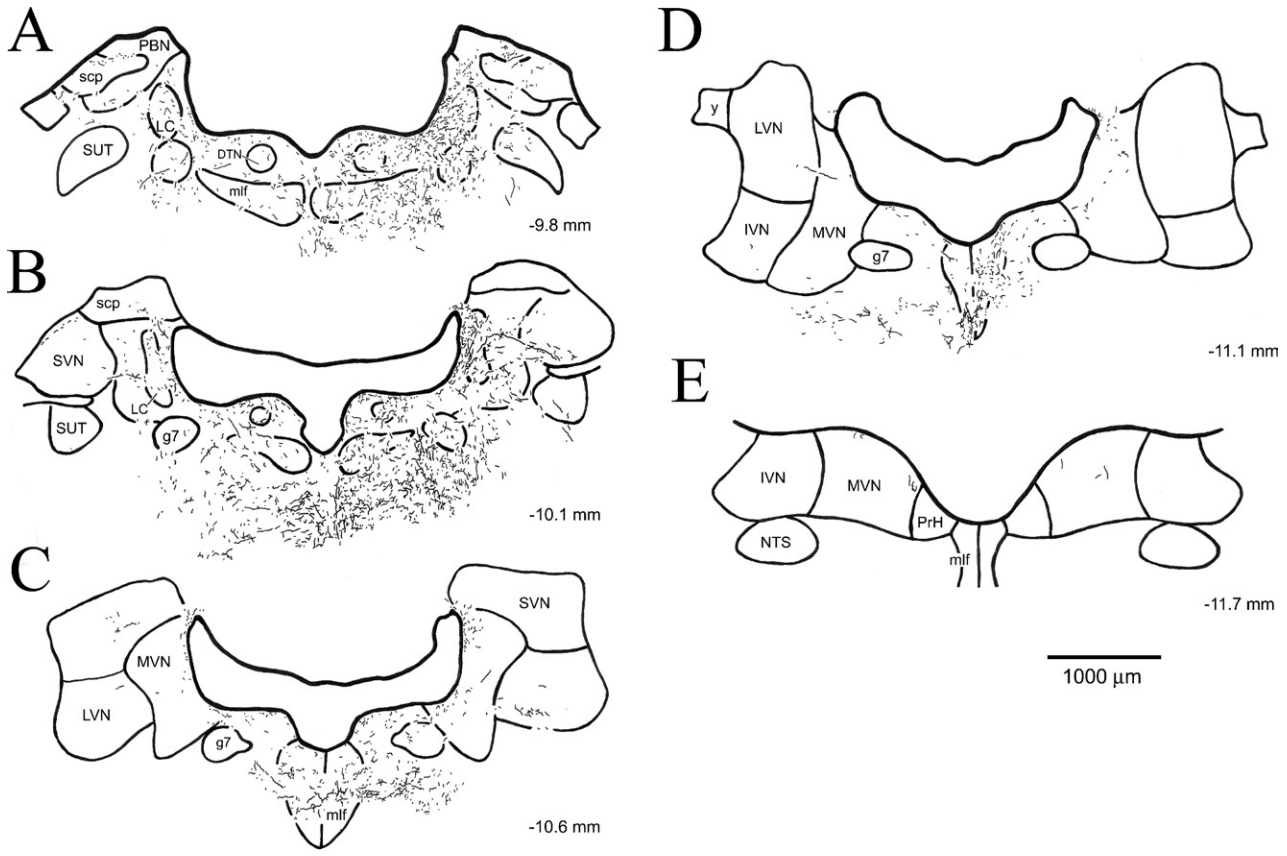

Fig. 4. Distribution of anterogradely labeled fibers in a series of transverse sections spanning the rostrocaudal extent of the vestibular nuclei from case DHT-222C. BDA-labeled fibers are charted in camera lucida drawings of five progressively caudal sections (A–E) located at the indicated AP level (relative to bregma). Transport ipsilateral to the injection site is illustrated on the right side of the figure. (Abbreviations: DTN, dorsal tegmental nucleus; g7, genu of facial nerve; NTS, nucleus tractus solitarius; PBN, parabrachial nucleus; PrH, nucleus prepositus hypoglossi; scp, superior cerebellar peduncle; sg, supragenual nucleus; SLC, nucleus subcoeruleus; SUT, supratrigeminal nucleus; y, group y).

presence of a 5,7-DHT injection site could not be verified using 5-HT immunostaining *and* by at least one of the latter two methodologies were treated as control injections for purposes of analysis. Of the 16 5,7-DHT-injected animals analyzed for this study, 13 met the criteria for verification that the 5,7-DHT injection site was located within the DRN. In each of the 13 cases, the location of the 5,7-DHT injection site within the DRN was detectable using all three criteria (5-HT immunostaining, silver staining, and Fluoro-Jade B staining). The three remaining cases, DHT-01, DHT-15, and DHT-16, served as control injection cases for purposes of comparison.

Effect of local administration of 5,7-DHT on 5-HT immunostaining. The effects of local microinjection of 5,7-DHT on the distribution of 5-HT-positive cell bodies in the DRN were examined using 5-HT immunostaining. In control animals, numerous 5-HT-immunopositive perikarya were scattered throughout the DRN within the dorsomedial, ventromedial, and lateral subdivisions (Fig. 6A, B). After injection of 5,7-DHT directly into the DRN, the location of the injection site was clearly discernable as a region in which somatodendritic 5-HT immunostaining was reduced markedly in intensity or even completely eliminated (Fig. 6C–F).

In control animals, a mixture of fine caliber and heavier caliber 5-HT-positive fibers was observed within the vestibular nuclei (Fig. 7A). This labeling was present throughout the vestibular nuclei, but it was much weaker in IVN compared with MVN, SVN and LVN. Importantly, microinjection of 5,7-DHT into the DRN resulted in a profound loss of 5-HT-immunoreactive fibers within terminal regions (Fig. 7B). The 5-HT-immunopositive fibers that were spared by treatment with 5,7-DHT were typically of heavy caliber.

Fluoro-Jade B staining of degenerating DRN neurons. Fluoro-Jade B-positive neurons were detected in the DRN (Fig. 8A). The neurons labeled with Fluoro-Jade B exhibited a bright yellow–green fluorescence under epifluorescence illumination. In control animals, no DRN neurons were stained with Fluoro-Jade B. The distribution of Fluoro-Jade B-positive neurons within the DRN (Fig. 8A) closely matched the location of argyrophilic neurons in adjacent sections that had been stained using the amino–cupric–silver technique (Fig. 8C–E). Furthermore, the morphologic appearance of Fluoro-Jade B-positive neurons and argyrophilic neurons was similar to that of 5-HT-positive neurons from the DRN of normal animals (Fig. 8B), and the Fluoro-Jade B-positive neurons and

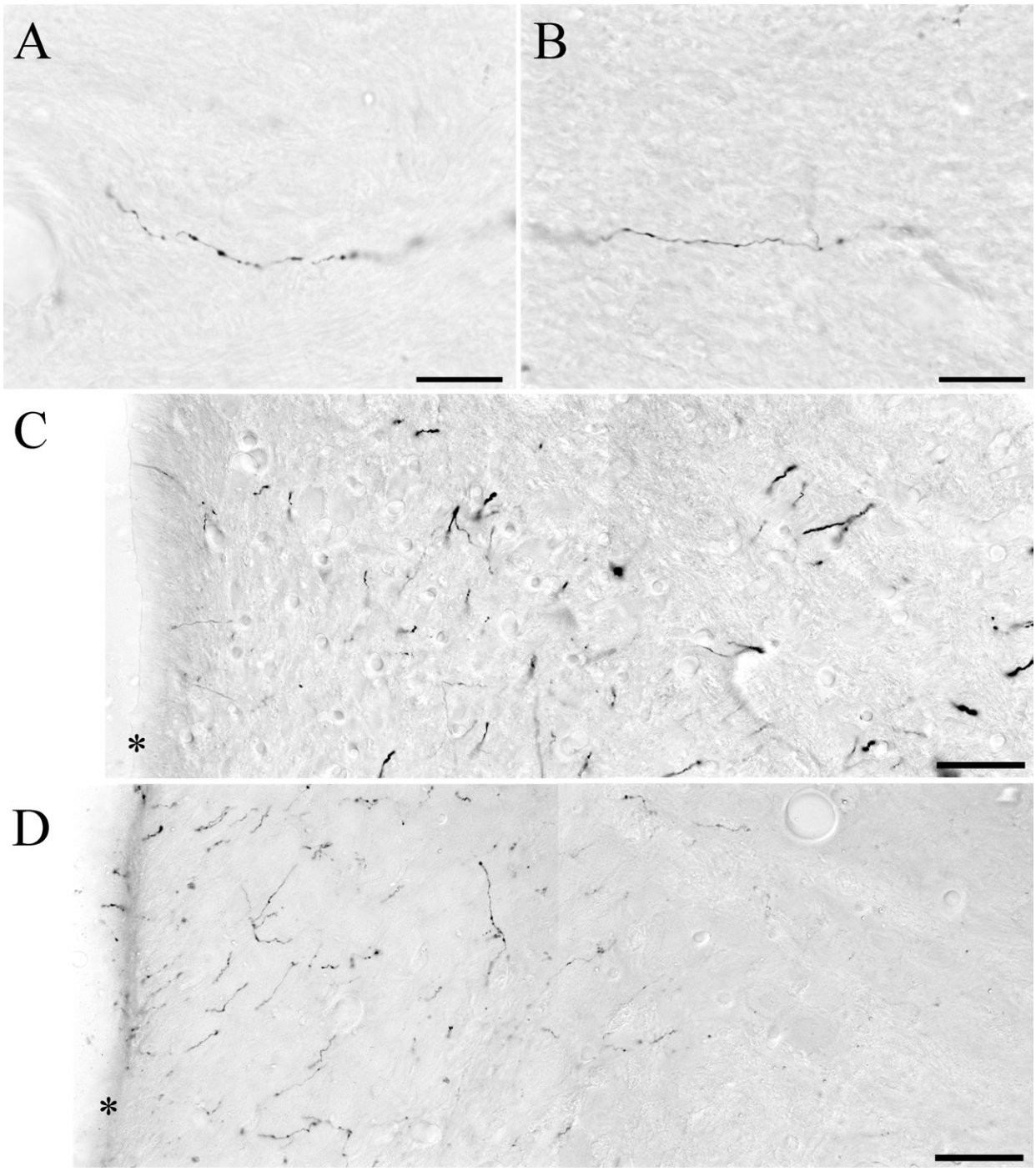

Fig. 5. Photomicrographs of BDA-labeled fibers and terminals within the vestibular nuclei. (A) Example of a fine caliber varicose fiber in SVN. (B) Example of a fine caliber varicose fiber in MVN. (C) Distribution of BDA anterograde labeling in MVN of a normal animal. This data were obtained from a previous anterograde tracing experiment (see Halberstadt and Balaban, 2006b). The border of the fourth ventricle is denoted with an asterisk. Note the presence of heavier caliber labeled fibers within the lateral aspect of MVN. (D) Distribution of BDA anterograde labeling in MVN in a 5,7-DHT-pretreated animal. Labeled fibers extend laterally from the ventricular plexus (indicated by the asterisk), innervating the medial aspect of MVN. Note that much less anterograde labeling is present further laterally in MVN. Also note the complete absence of heavier caliber fiber labeling within MVN. Scale bars=20 μm in A and B, and 50 μm in C and D.

argyrophilic neurons were located within regions of DRN where serotonergic cells are known to be clustered heavily.

Amino–cupric–silver staining: Somatodendritic degeneration in DRN. Argyrophilic neurons, as well as a substantial amount of dendritic and terminal debris, were ap-

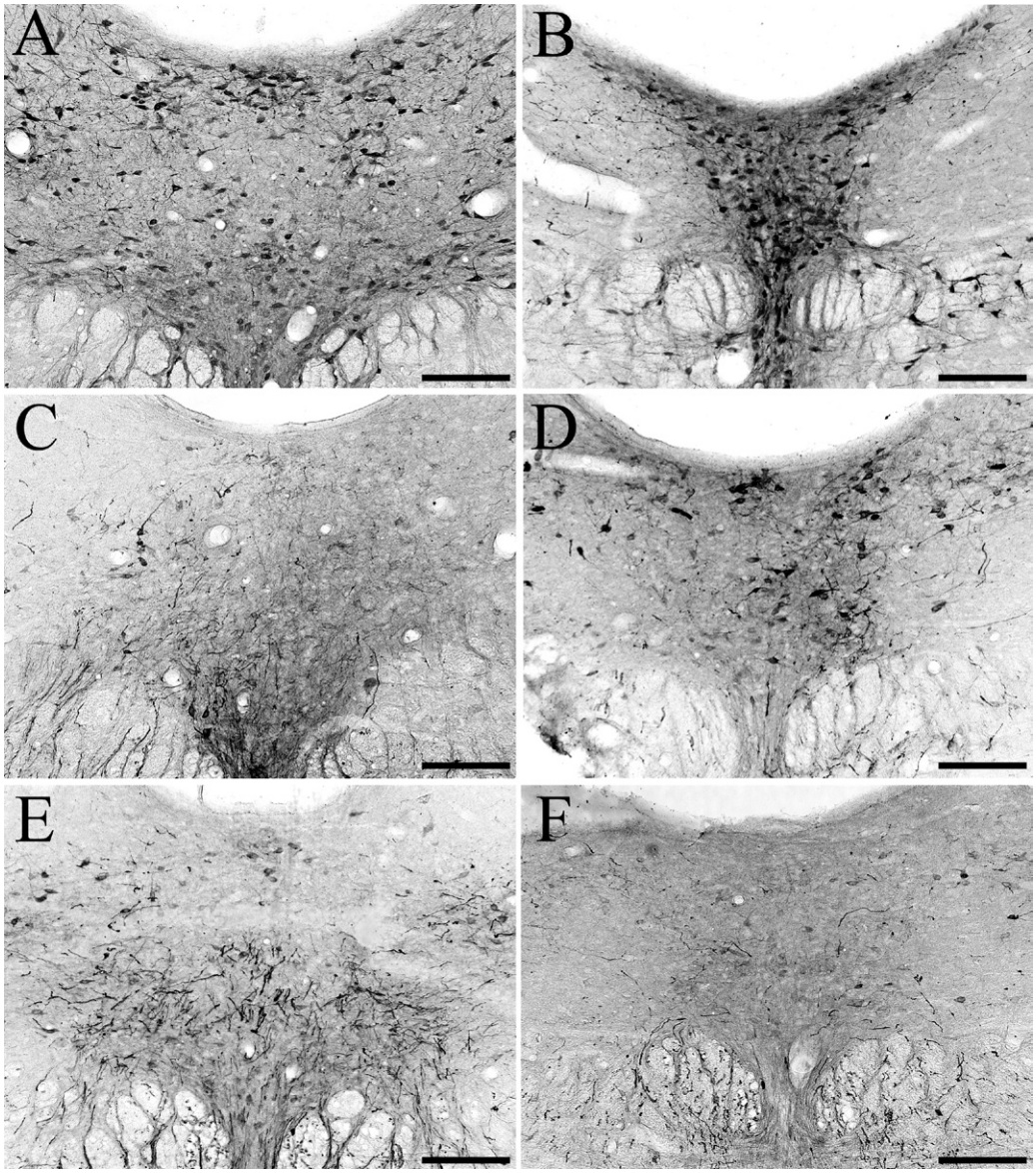

Fig. 6. 5-HT immunostaining in the DRN of control animals (A,B) and in animals in which 5,7-DHT was injected into the DRN (C-F). A section from mid-level DRN (A, C, E) and from caudal DRN (B, D, F) is shown for each animal. (A, B) In control animals, numerous 5-HT-positive cell bodies are localized throughout DRN. (C, D) After injection of 5,7-DHT into the DRN in case DHT-02, the reduction in 5-HT immunostaining was heaviest in the dorsomedial and lateral subdivisions of mid-level DRN. (E, F) After injection of 5,7-DHT into the DRN in case DHT-04, the reduction in 5-HT immunostaining was heaviest in caudal DRN and the dorsomedial aspect of mid-level DRN. Scale bars=200 μm.

parent in the DRN after local microinjection of 5,7-DHT. Most degenerating neurons were partially or completely filled with very fine silver granules (Fig. 8C–E), although a few degenerating neurons were impregnated densely and had a Golgi-like appearance. There was substantial case-by-case variation in the number and distribution of degenerating DRN neurons. In some injection cases, small numbers of degenerating neurons were found localized within an individual DRN subdivision. For example, neuronal degeneration was primarily confined to DRNvm in case DHT-02, and in case DHT-14 degenerating neurons were located in DRNdm. However, in the majority of injection cases, relatively large numbers of argyrophilic neurons were distributed over a substantial mediolateral, dorsoventral and rostrocaudal region of the DRN.

Amino–cupric–silver staining: Degeneration in the descending mlf and ventricular plexus pathways. After injection of 5,7-DHT into the DRN, no degenerating fibers were observed within the mlf at the short survival time (18 h) used in these experiments. However, degenerating fibers followed the course of DRN efferents between the mlf and the vestibular nuclei. Conversely, large numbers of fine-caliber degenerating fibers and terminals were present adjacent to the fourth ventricle within the ventricular and periventricular plexus.

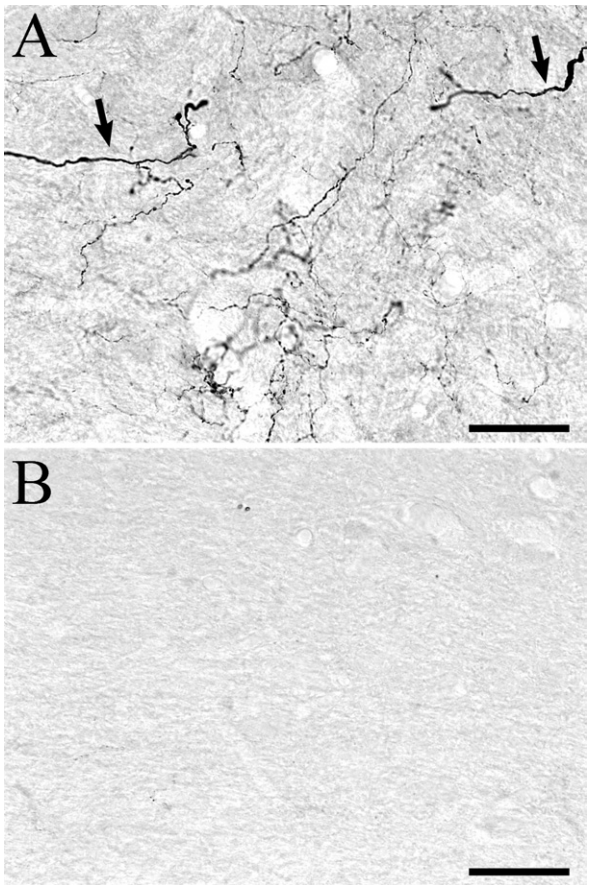

Fig. 7. 5-HT immunostaining in MVN from a control animal (A) and in MVN from an animal in which 5,7-DHT was injected into the DRN (B). (A) In control animals, regions of the vestibular nuclei are innervated by a mixture of heavier caliber 5-HT positive fibers (indicated by arrows) and fine caliber 5-HT positive fibers. (B) There are very few 5-HT-immunopositive fibers in the vestibular nuclei after injection of 5,7-DHT into the DRN. Note that sections from control and 5,7-DHT-pretreated animals were immunostained for 5-HT simultaneously. Scale bars=50 μm.

Amino–cupric–silver staining: Terminal degeneration in the vestibular nuclei. There was extensive axonal and terminal degeneration within the vestibular nuclei in animals that received a 5,7-DHT microinjection in DRN. The degeneration was found in the rostral (Fig. 9) and caudal (Fig. 10) aspects of the vestibular nuclei, predominantly in regions corresponding to the location of the rostrodorsal and caudoventral terminal fields revealed using BDA tracing (see Halberstadt and Balaban, 2006b).

In the rostral half of the vestibular nuclei, silver-impregnated terminals were present in SVN (Fig. 9A), LVN (Fig. 9B), and MVN (Fig. 9C, D). Extensive terminal degeneration was localized in SVN, and these terminals were typically of fine caliber (Fig. 9A). Heavier caliber degenerating terminals were distributed sparsely in rostral LVN (Fig. 9B). A substantial plexus of fine caliber degenerating terminals was located in the ventricular plexus, including the part of the ventricular plexus that borders rostral MVN (Fig. 9C). In the medial aspect of rostral MVN, degenerating terminals extended laterally from the ventricular plexus to innervate the medial aspect of MVN. Further laterally in rostral MVN, there was a dense plexus of degeneration, involving both fine caliber and heavier caliber terminals (Fig. 9D).

In the caudal half of the vestibular nuclei, silver-impregnated terminals were prominent in caudal LVN (Fig. 10A) and caudal MVN (Fig. 10B–D). Relatively sparse degeneration was present in caudal LVN (Fig. 10A). However, although only heavier caliber degenerating terminals were located in rostral LVN, there was a mixture of both fine and heavier caliber degeneration in caudal LVN. Degenerating, fine caliber terminals were found in the ventricular plexus adjacent to caudal MVN (Fig. 10B), but the density of these fibers was not as high as was found at more rostral levels of the vestibular nuclei. In particular, terminals in the ventricular plexus ramified laterally into the medial aspect of caudal MVN (Fig. 10B). The lateral aspect of caudal MVN contained a mixture of fine caliber and heavier caliber terminal degeneration (Fig. 10C, D). Within both the rostral and caudal aspects of IVN, there was little or no terminal degeneration (data not shown).

DISCUSSION

Distinct serotonergic and nonserotonergic components of DRN projections to the vestibular nuclei

This study presents the first evidence that serotonergic and nonserotonergic components of DRN projections to the vestibular nuclei are distinct anatomic pathways. Anterograde tracing data indicate that axons of nonserotonergic and serotonergic DRN neurons are distributed differentially in two fiber pathways, the ventricular and periventricular plexus and the mlf. Further, these data demonstrate clearly that serotonergic and nonserotonergic axons innervate distinct but partially overlapping fields within vestibular nuclei. This section discusses the characteristic features of these pathways.

Serotonergic and nonserotonergic fiber pathways from DRN to the vestibular nuclei. The results of our previous BDA anterograde tracing studies demonstrate that DRN gives rise to (1) fine caliber fibers that descend to the vestibular nuclei within the ventricular and periventricular plexus, and (2) heavier caliber fibers that descend to the vestibular nuclei within the mlf (Halberstadt and Balaban, 2006b). The DRN fibers in the ventricular and periventricular plexuses are fine caliber axons that innervate the periventricular regions of MVN. The mlf pathway contributes heavier caliber axons to distinct rostrodorsal and caudoventral vestibular terminal fields. Conversely, as shown in the present report, injection of BDA into the DRN of animals that were pretreated with 5,7-DHT produced labeled fibers that descended to the vestibular nuclei within the ventricular plexus but not within the mlf. Thus, many fibers descending in the ventricular plexus DRN projection pathway were *spared* by 5,7-DHT treatment, but fibers descending in the mlf DRN projection pathway were *completely eliminated*. These findings, combined with the loss of SERT immunoreactive heavy caliber axons in the mlf after 5,7-DHT administration, suggest strongly that the

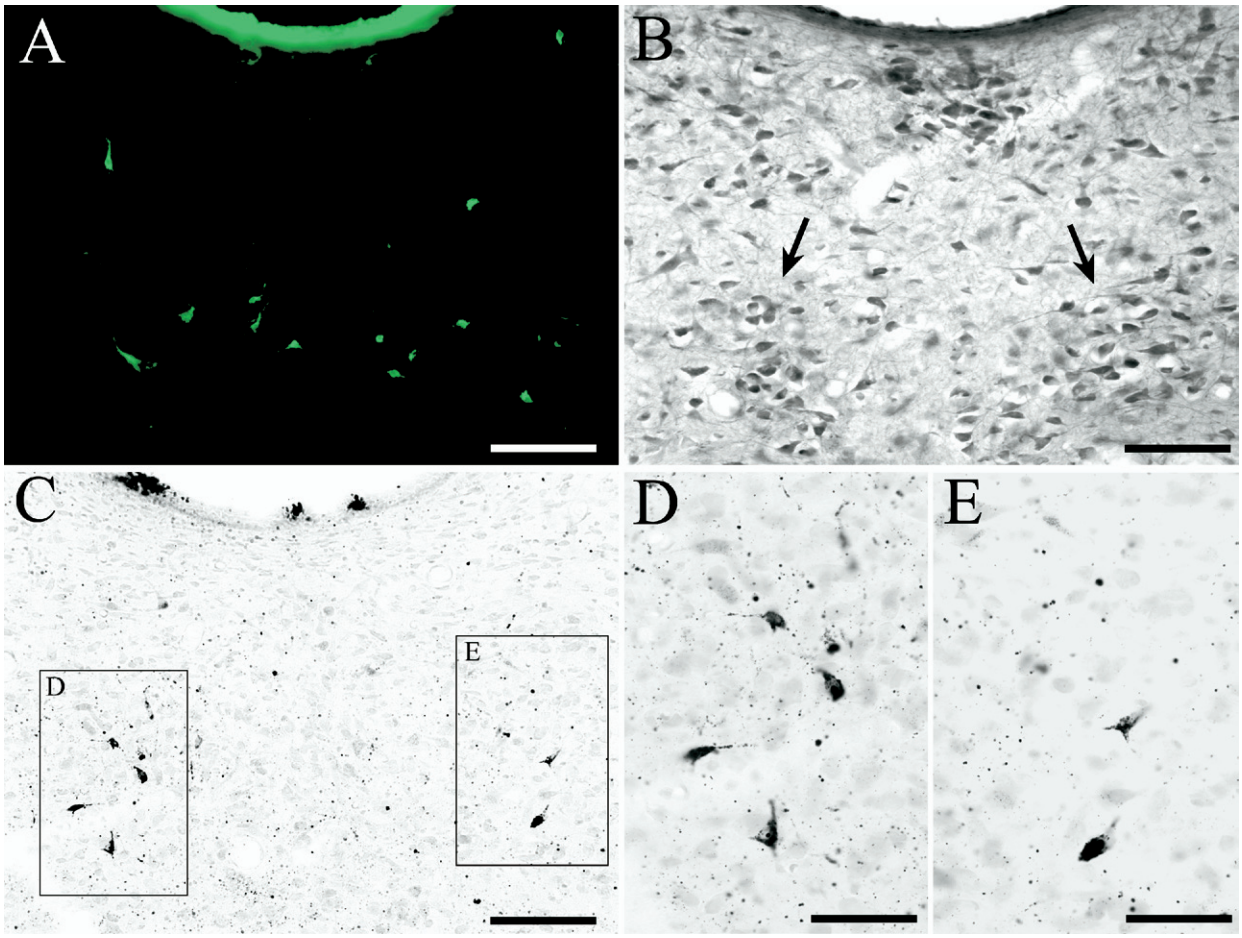

Fig. 8. After injection of 5,7-DHT into the DRN, degenerating neurons are located in regions of DRN where 5-HT immunopositive neurons are normally heavily clustered. (A) Fluoro-Jade B staining in the DRN of 5,7-DHT injection case DHT-04. Several Fluoro-Jade B-stained neurons are located within the dorsomedial DRN subdivision, especially the ventral half of DRNdm. (B) Distribution of 5-HT immunopositive neurons within DRNdm of a control animal. Within the ventral aspect of DRNdm, 5-HT positive cells are heavily clustered within two lateral groups (indicated by arrows). (C) Amino–cupric–silver staining in DRNdm from case DHT-04; this section was located adjacent to the section in panel A. There are two clusters of densely silver-impregnated cells in ventral DRNdm. Note that the distribution of these argyrophilic neurons is similar to that of the Fluoro-Jade B-stained cells in panel A. Also note that these argyrophilic neurons are located within the same region of ventral DRNdm where 5-HT positive neurons are heavily clustered (see panel B). The boxes in panel C indicate the areas shown enlarged in panels D and E. (D, E) High-power photomicrographs showing the morphology of argyrophilic somata in the same DRN section as panel C. Scale bars=100 μm in A, B and C, and 50 μm in D and E.

DRN-vestibular nucleus fibers in the mlf arise *exclusively* from serotonergic DRN cells.

By contrast, the ventricular and periventricular plexus appears to contain both nonserotonergic and serotonergic DRN projections. Presumptive non-serotonergic fine caliber DRN projections persisted within the ventricular and periventricular plexus after administration of 5,7-DHT. The silver degeneration results after local 5,7-DHT administration and the immunohistochemical results also revealed a serotonergic contingent of axons in the ventricular and periventricular plexus. Hence, there are two descending pathways from DRN to the vestibular nuclei, (1) a serotonergic and nonserotonergic fine caliber pathway via the ventricular and periventricular plexus and (2) an exclusively serotonergic large caliber pathway via the mlf.

Differential distribution of serotonergic and non-serotonergic terminal fields in the vestibular nuclei. The nonserotonergic and serotonergic DRN projections appear to terminate within three distinct, although overlapping, terminal regions within the vestibular nuclei. The anatomical localization of these three terminal regions—the periventricular field, the rostrodorsal field, and the caudoventral field—is illustrated in Fig. 11. The periventricular vestibular terminal field includes SVN and the region of MVN that borders the fourth ventricle. It receives fine caliber serotonergic and nonserotonergic fibers that descend from the DRN within the ventricular plexus. By contrast, both the rostrodorsal and the caudoventral serotonergic terminal regions receive projections from distinct bundles of larger caliber fibers that descend in the mlf (Halberstadt and Balaban, 2006b), and involve both the medial and lateral aspects of the vestibular nuclei. Thus, there appear to be two organizational systems of DRN–vestibular nucleus pathways. Overlapping serotonergic and nonserotonergic projections provide small caliber fibers to the SVN and periventricular aspect of the MVN via the ventricular and

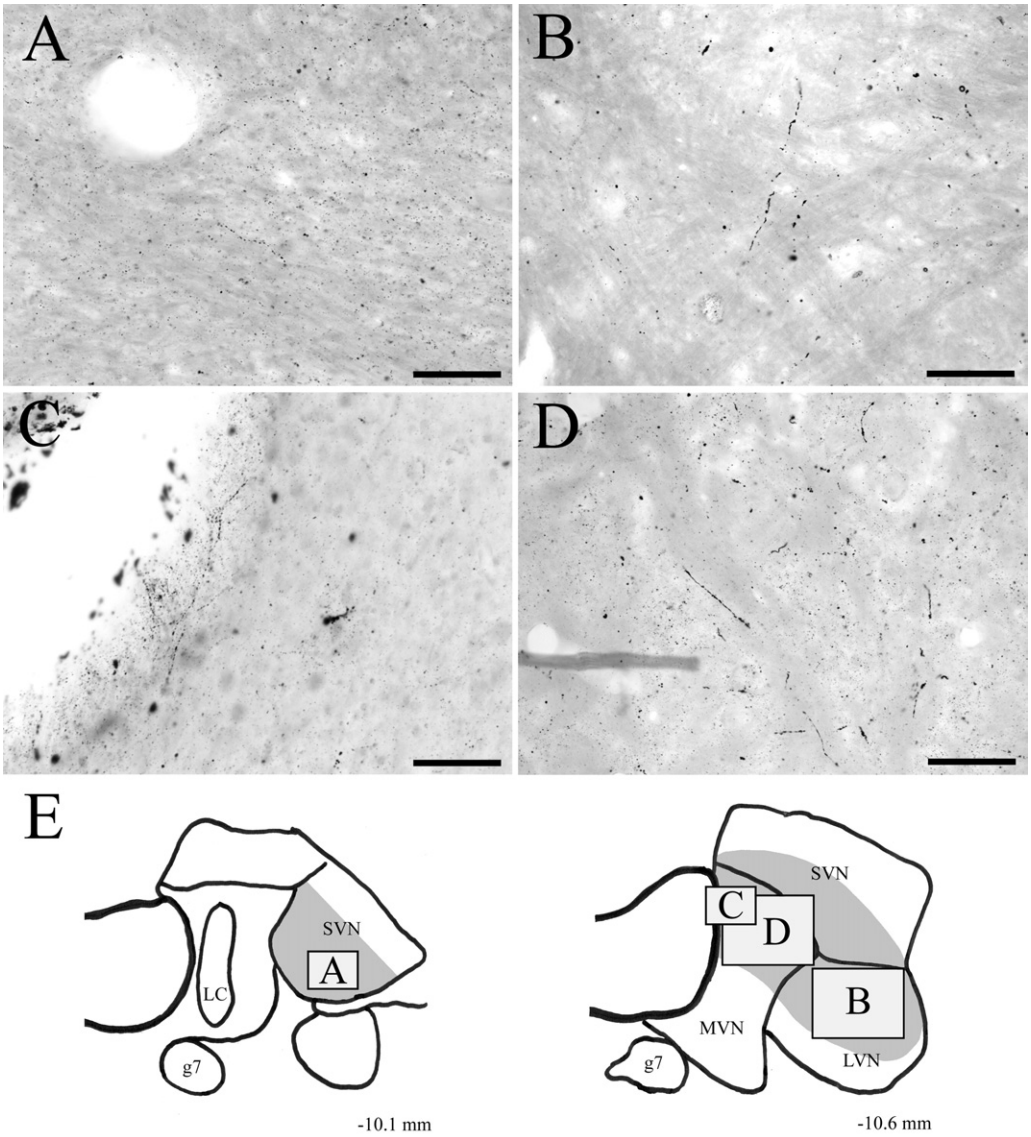

Fig. 9. Photomicrographs of amino–cupric–silver-stained sections illustrating axonal debris in the rostrodorsal vestibular terminal region, 18 h after injection of 5,7-DHT into DRN. (A) Fine caliber axon terminal debris in rostral SVN. (B) Degenerating heavier caliber axons and axonal debris in rostrodorsal LVN. (C) Fine caliber terminal degeneration in the ventricular plexus and the adjacent periventricular region of rostrodorsal MVN. (D) The lateral aspect of rostrodorsal MVN contains a mixture of fine and heavier caliber degenerating axons and axonal debris. (E) Drawings of the rostral half of the vestibular nuclei illustrating the locations of panels A, B, C and D within the rostrodorsal terminal field, which is shaded in gray. Note that the four photomicrographs are from sections at or near the indicated AP level (relative to bregma), and are from different injection cases. Scale bars=50 μm in A and C, and 100 μm in B and D.

periventricular plexus. The second serotonergic system is a large caliber projection via the mlf to the rostrodorsal and caudoventral DRN terminal fields.

Organization of DRN projections to the vestibular nuclei

The segregation of fine caliber and heavier caliber serotonergic fibers in distinct pathways is a striking organizational feature of DRN-to-vestibular nucleus projections. Comparisons of the pattern of BDA anterograde labeling in normal animals and in animals pretreated with 5,7-DHT indicated that the heavier caliber serotonergic DRN projections descend to the vestibular nuclei exclusively within the mlf pathway. The results of the silver staining experiments demonstrated further that the fine caliber serotonergic DRN projections descend to the vestibular nuclei within the ventricular plexus (see Figs. 9C and 10B). Since fine caliber nonserotonergic projections are distributed in the same pattern as fine caliber serotonergic fibers, these findings indicate that DRN may have at least two functional output components. A slower conducting DRN pathway via the ventricular and periventricular plexus appears likely produce effects via a convergence of parallel serotonergic and nonserotonergic signals in a region centered in SVN

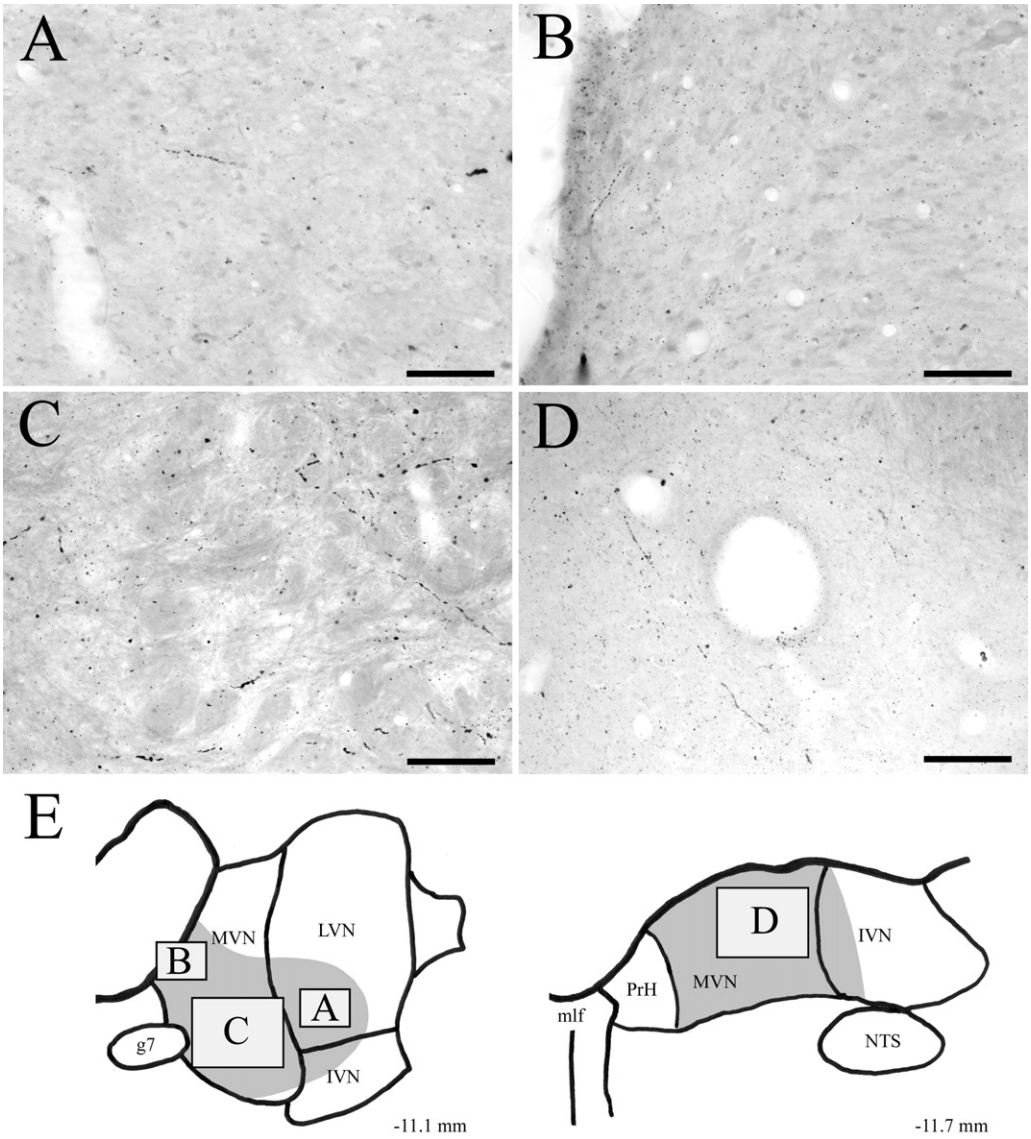

Fig. 10. Photomicrographs of amino–cupric–silver-stained sections illustrating axonal debris in the caudoventral vestibular terminal region, 18 h after injection of 5,7-DHT into DRN. (A) Fine and heavier caliber degeneration in caudal LVN. (B) Fine caliber terminal degeneration in the ventricular plexus and the adjacent periventricular region of ventral MVN. Note the presence of terminals coursing laterally from the ventricular plexus into medial MVN. (C) The lateral aspect of ventral MVN contains a mixture of fine and heavier caliber degenerating axons and axonal debris. (D) Fine and heavier caliber debris in lateral caudal MVN. (E) Drawings of the caudal half of the vestibular nuclei illustrating the locations of panels A, B, C and D within the caudoventral terminal field, which is shaded in gray. Note that the four photomicrographs are from sections at or near the indicated AP level (relative to bregma), and are from different injection cases. Scale bars=50 μm in A and B, and 100 μm in C and D.

and the periventricular aspect of MVN. By contrast, a faster conducting DRN pathway via the mlf is likely to produce purely serotonergic effects in MVN, SVN and LVN.

There is extensive evidence that there is a volume or paracrine component to serotonergic transmission (Bunin and Wightman, 1998, 1999; Zhou et al., 1998), and the presence of SERT on extrasynaptic axon segments indicates that SERT may act to regulate 5-HT volume transmission (Zhou et al., 1998). It has been reported that heavier caliber 5-HT-immunopositive fibers in ascending serotonergic projections do not co-localize SERT (Brown and Molliver, 2000; Nielsen et al., 2006). This may be a consistent feature of heavier caliber serotonergic fibers because we observed heavier caliber fibers in lateral regions of the vestibular nuclei with 5-HT immunohistochemistry (see Fig. 11), but only identified small caliber fibers with SERT immunohistochemistry (Halberstadt and Balaban, 2003). This may have important functional implications for the small and larger caliber serotonergic DRN–vestibular nuclear pathways. The SERT expression by fine caliber axons in medial MVN and SVN may indicate that actions of 5-HT are focused locally; SERT activation would tend to limit diffusion of 5-HT from synapses within the periventricular field. Conversely, the absence of SERT immunoreactivity within the heavier caliber serotonergic innervation raises the possibility that 5-HT transmission is

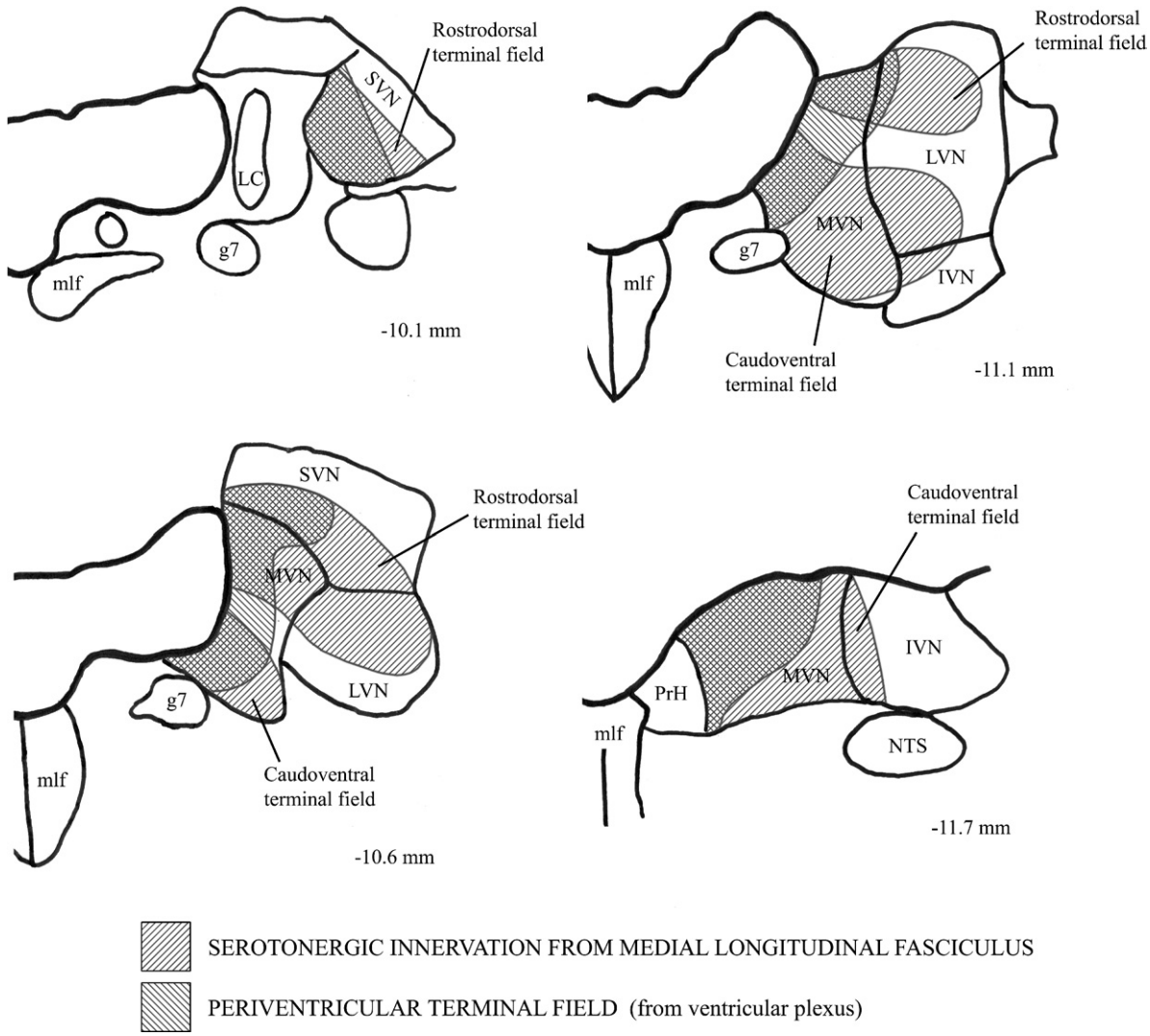

Fig. 11. Illustration of the location of the periventricular, rostrodorsal, and caudoventral DRN terminal fields within the vestibular nuclei. The periventricular terminal field is targeted by fine caliber serotonergic and nonserotonergic fibers that descend from the DRN within the ventricular plexus. The rostrodorsal terminal field and the caudoventral terminal field are targeted by heavier caliber serotonergic fibers that descend from the DRN within the mlf. (Abbreviations: g7, genu of facial nerve; NTS, nucleus tractus solitarius; PrH, nucleus prepositus hypoglossi.)

much more paracrine in the regions of the vestibular nuclei that are innervated by the large caliber DRN projection though the mlf.

Different functional regions of the vestibular nuclei appear to receive different combinations of serotonergic and non-serotonergic DRN inputs and noradrenergic inputs from the coeruleovestibular pathway (Schuerger and Balaban, 1999). Lateral vestibulospinal tract neurons in the dorsal aspect of the LVN receive a large caliber serotonergic projection and a heavy noradrenergic projection from LC. On the other hand, regions of the medial and superior vestibular nuclei that receive nodulus input (Xiong and Matsushita, 2000) receive prominent projections from small caliber serotonergic and non-serotonergic DRN afferents and an intermediate density of noradrenergic innervation from LC. The regions of the vestibular nuclei that receive flocculus input, by contrast, receive little input from either DRN or LC. Finally, the regions of the SVN that project to the parabrachial nucleus (Porter and Balaban, 1997) receive small caliber serotonergic and non-serotonergic DRN afferents, large caliber serotonergic DRN afferents, and intermediate-to-heavy noradrenergic innervation from LC. This degree of diversity in organization likely provides a basis for nuanced differential monoaminergic regulation of vestibular function.

The co-localization of small caliber serotonergic and non-serotonergic DRN projections raises the question of possible types of interactions between these axons. To our knowledge, there is no information regarding interactions between serotonergic and nonserotonergic DRN fibers terminals in a given target region. However, there is evidence that serotonergic and nonserotonergic neurons interact within the DRN. Electrophysiological evidence indicates that glutamatergic DRN cells (Jolas and Aghajanian, 1997; Liu et al., 2002a) and GABAergic DRN cells (Liu et al., 2000, 2002b) send projections to serotonergic DRN neu-

rons. Conversely, although it was reported initially that the only DRN neurons that express 5-HT_{1A} receptor immunoreactivity are serotonergic (Sotelo et al., 1990), more recent findings have revealed that nonserotonergic DRN neurons also express 5-HT_{1A} receptors (Kirby et al., 2003; Day et al., 2004). Indeed, several recent *in vitro* electrophysiological studies have demonstrated that 5-HT- and tryptophan hydroxylase (TPH)-immunonegative DRN neurons respond to bath application of 5-HT_{1A} agonists (Kirby et al., 2003; Beck et al., 2004; Marinelli et al., 2004). Furthermore, most GABAergic DRN neurons express 5-HT_{2C} receptor mRNA (Serrats et al., 2005), and there is evidence that the selective 5-$HT_{2A/2C}$ agonist 1-(2,5-dimethoxy-4-iodophenyl)-2-aminopropane (DOI) can excite putative GABAergic DRN neurons (Liu et al., 2000; see also Marinelli et al., 2004). Evidence has also been presented which indicates that GABAergic and serotonergic DRN neurons are reciprocally interconnected (Bagdy et al., 2000). These findings indicate that there is substantial mutual feed-forward regulation between serotonergic and nonserotonergic neurons in the DRN. However, it is an open question as to whether analogous interactions occur on neurons in the vestibular nuclei.

CONCLUSION

The results of these experiments provide the first evidence that the serotonergic and nonserotonergic DRN projections represent distinct projection systems. Although it has been known for some time that DRN projections arise from both serotonergic and nonserotonergic cells, there is little evidence regarding the comparative distribution of these projections within individual target regions. After injecting *Phaseolus vulgaris* leucoagglutinin into the DRN of two rats, Kosofsky and Molliver (1987) used 5-HT immunofluorescence staining to compare the organization of serotonergic and nonserotonergic DRN projections within regions of cerebral cortex. They reported that anterogradely labeled 5-HT-positive and 5-HT-negative axons were found clustered together in cortex and that only 5–20% of the axons were nonserotonergic. A similar study was conducted by Aznar et al. (2004), using a combination of 5-HT immunofluorescence staining and injections of BDA into the DRN. They found that 86% of the BDA-labeled fibers in the lateral septum, 90% of the BDA-labeled fibers in the medial septum, and 83% of the BDA-labeled fibers in the diagonal band of Broca were nonserotonergic. However, both the serotonergic and nonserotonergic fibers projected onto calbindin- and parvalbumin-positive cells within the septum. Thus, these previous studies indicated that serotonergic and nonserotonergic DRN projections are often colocalized in target regions, but that they differ in relative density of terminations in each region. By contrast, our data demonstrate that within at least one particular target region there is not complete overlap between these two projections. Therefore, rather than treating the DRN as a single projection system containing both serotonergic and nonserotonergic components, it may be more accurate to treat it as two separate projection systems that originate from within the same nucleus.

These experiments have also revealed a number of previously unknown features of the organization of projections from DRN to the vestibular nuclei. Although it was previously demonstrated that both serotonergic and nonserotonergic DRN neurons project to the vestibular nuclei (Halberstadt and Balaban, 2003, 2006a), it is now apparent that there are pronounced differences in the terminal distribution of these two projections. Additionally, the serotonergic component of the DRN projection to the vestibular nuclei appears to be heterogeneous with regard to the caliber of the axons, expression of SERT, and trajectory in the lower brainstem. It is also clear that the terminals of DRN projections are distributed within three partially overlapping fields within the vestibular nuclei. The fact that DRN innervation of the vestibular nuclei is distributed in multiple terminal fields indicates that this projection may be organized to selectively and differentially modulate processing within particular vestibular pathways. In particular, the location of the three terminal fields within the vestibular nuclei indicates that these projections are organized to influence processing in vestibular regions involved in eye movement, velocity storage, vestibular–autonomic interactions, and postural responses (for further discussion, see Halberstadt and Balaban, 2006b).

Acknowledgments—This work was supported in part by NIDCD grants R01 DC00739 and F31 DC006772. We would like to thank Gloria Limetti and Jean Betsch for their excellent technical assistance.

REFERENCES

Aghajanian GK, Wang RY, Baraban J (1978) Serotonergic and nonserotonergic neurons of the dorsal raphe: reciprocal changes in firing induced by peripheral nerve stimulation. Brain Res 153:169–175.

Araneda S, Bobillier P, Buda M, Pujol JF (1980a) Retrograde axonal transport following injection of [^{3}H]serotonin in the olfactory bulb. I. Biochemical study. Brain Res 196:405–415.

Araneda S, Gamrani H, Font C, Calas A, Pujol JF, Bobillier P (1980b) Retrograde axonal transport following injection of [^{3}H]serotonin into the olfactory bulb. II. Radioautoradiographic study. Brain Res 196:417–427.

Azmitia EC, Segal M (1978) An autoradiographic analysis of the differential ascending projections of the dorsal and median raphe nuclei in the rat. J Comp Neurol 179:641–667.

Aznar S, Qian ZX, Knudsen GM (2004) Non-serotonergic dorsal and median raphe projection onto parvalbumin- and calbindin-containing neurons in hippocampus and septum. Neuroscience 124: 573–581.

Bagdy E, Kiraly I, Harsing LG Jr (2000) Reciprocal innervation between serotonergic and GABAergic neurons in the raphe nuclei of the rat. Neurochem Res 25:1465–1473.

Balaban CD (2002) Neural substrates linking balance control and anxiety. Physiol Behav 77:469–475.

Balaban CD, Thayer JF (2001) Neurological bases for balance-anxiety links. J Anxiety Disord 15:53–79.

Baumgarten HG, Klemm HP, Sievers J, Schlossberger HG (1982) Dihydroxytryptamines as tools to study the neurobiology of serotonin. Brain Res Bull 9:131–150.

Beck SG, Pan YZ, Akanwa AC, Kirby LG (2004) Median and dorsal raphe neurons are not electrophysiologically identical. J Neurophysiol 91:994–1005.

Beitz AJ, Clements JR, Mullett MA, Ecklund LJ (1986) Differential origin of brainstem serotonergic projections to the midbrain periaqueductal gray and superior colliculus of the rat. J Comp Neurol 250:498–509.

Bendotti C, Servadio A, Forloni G, Angeretti N, Samanin R (1990) Increased tryptophan hydroxylase mRNA in raphe serotonergic neurons spared by 5,7-dihydroxytryptamine. Mol Brain Res 8: 343–348.

Björklund A, Baumgarten HG, Rensch A (1975) 5,7-Dihydroxytryptamine: improvement of its selectivity for serotonin neurons in the CNS by pretreatment with desipramine. J Neurochem 24: 833–835.

Brown P, Molliver ME (2000) Dual serotonin (5-HT) projections to the nucleus accumbens core and shell: relation of the 5-HT transporter to amphetamine-induced neurotoxicity. J Neurosci 20:1952–1963.

Bunin MA, Wightman RM (1998) Quantitative evaluation of 5-hydroxytryptamine (serotonin) neuronal release and uptake: an investigation of extrasynaptic transmission. J Neurosci 18:4854–4860.

Bunin MA, Wightman RM (1999) Paracrine neurotransmission in the CNS: involvement of 5-HT. Trends Neurosci 22:377–382.

Caillé S, Espejo EF, Koob GF, Stinus L (2002) Dorsal and median raphe serotonergic system lesion does not alter the opiate withdrawal syndrome. Pharmacol Biochem Behav 72:979–986.

Callahan BT, Cord BJ, Ricaurte GA (2001) Long-term impairment of anterograde axonal transport along fiber projections originating in the rostral raphe nuclei after treatment with fenfluramine or methylenedioxyamphetamine. Synapse 40:113–121.

Commins DL, Axt KJ, Vosmer G, Seiden LS (1987a) Endogenously produced 5,6-dihydroxytryptamine may mediate the neurotoxic effects of para-chloroamphetamine. Brain Res 419:253–261.

Commins DL, Vosmer G, Virus RM, Woolverton WL, Schuster CR, Seiden LS (1987b) Biochemical and histological evidence that methylenedioxymethylamphetamine (MDMA) is toxic to neurons in the rat brain. J Pharmacol Exp Ther 241:338–345.

Dahlström A, Fuxe K (1964) Evidence for the existence of monoamine-containing neurons in the central nervous system. I. Demonstration of monoamines in cell bodies of brain stem neurons. Acta Physiol Scand 62 (Suppl 232):1–55.

Datiche F, Luppi PH, Cattarelli M (1995) Serotonergic and non-serotonergic projections from the raphe nuclei to the piriform cortex in the rat: a cholera toxin B subunit (CTb) and 5-HT immunohistochemical study. Brain Res 671:27–37.

Day HE, Greenwood BN, Hammack SE, Watkins LR, Fleshner M, Maier SF, Campeau S (2004) Differential expression of 5HT-1A, α_{1b} adrenergic, CRF-R1, and CRF-R2 receptor mRNA in serotonergic, γ-aminobutyric acidergic, and catecholaminergic cells of the rat dorsal raphe nucleus. J Comp Neurol 474:364–378.

de Olmos JS, Beltramino CA, de Olmos de Lorenzo S (1994) Use of an amino-cupric-silver technique for the detection of early and semiacute neuronal degeneration caused by neurotoxicants, hypoxia, and physical trauma. Neurotoxicol Teratol 16:545–561.

de Olmos JS, Ebbesson SOE, Heimer L (1981) Silver methods for the impregnation of degenerating axoplasm. In: Neuroanatomical tract-tracing methods (Heimer L, Robards MJ, eds), pp. 117–170. New York: Plenum Press.

Drummond PD (2005) Effect of tryptophan depletion on symptoms of motion sickness in migraineurs. Neurology 65:620–622.

Furman JM, Balaban CD, Jacob RG, Marcus DA (2005) Migraine-anxiety related dizziness (MARD): a new disorder? J Neurol Neurosurg Psychiatry 76:1–8.

Hajós M, Sharp T (1996) A 5-hydroxytryptamine lesion markedly reduces the incidence of burst-firing dorsal raphe neurons in the rat. Neurosci Lett 204:161–164.

Halaris AE, Jones BE, Moore RY (1976) Axonal transport in serotonin neurons of the midbrain raphe. Brain Res 107:555–574.

Halberstadt AL, Balaban CD (2003) Organization of projections from the raphe nuclei to the vestibular nuclei in rats. Neuroscience 120:573–594.

Halberstadt AL, Balaban CD (2006a) Serotonergic and nonserotonergic neurons in the dorsal raphe nucleus send collateralized projections to both the vestibular nuclei and the central amygdaloid nucleus. Neuroscience 140:1067–1077.

Halberstadt AL, Balaban CD (2006b) Anterograde tracing of projections from the dorsal raphe nucleus to the vestibular nuclei. Neuroscience 143:641–654.

Inazu M, Takeda H, Ikoshi H, Sugisawa M, Uchida Y, Matsumiya T (2001) Pharmacological characterization and visualization of the glial serotonin transporter. Neurochem Int 39:39–49.

Jacobs BL, Foote SL, Bloom FE (1978) Differential projections of neurons within the dorsal raphe nucleus of the rat: a horseradish peroxidase (HRP) study. Brain Res 147:149–153.

Jensen KF, Olin J, Haykal-Coates N, O'Callaghan J, Miller DB, de Olmos JS (1993) Mapping toxicant-induced nervous system damage with a cupric silver stain: a quantitative analysis of neural degeneration induced by 3,4-methylenedioxymethamphetamine. NIDA Res Monogr 136:101–132.

Johnson GD (1998) Medical management of migraine-related dizziness and vertigo. Laryngoscope 108 (Suppl 85):1–28.

Jolas T, Aghajanian GK (1997) Opioids suppress spontaneous and NMDA-induced inhibitory postsynaptic currents in the dorsal raphe nucleus of the rat in vitro. Brain Res 755:229–245.

Kim MA, Lee HS, Lee BY, Waterhouse BD (2004) Reciprocal connections between subdivisions of the dorsal raphe and the nuclear core of the locus coeruleus in the rat. Brain Res 1026:56–67.

Kirby LG, Pernar L, Valentino RJ, Beck SG (2003) Distinguishing characteristics of serotonin and non-serotonin-containing cells in the dorsal raphe nucleus: electrophysiological and immunohistochemical studies. Neuroscience 116:669–683.

Kirifides ML, Simpson KL, Lin RCS, Waterhouse BD (2001) Topographic organization and neurochemical identity of dorsal raphe neurons that project to the trigeminal somatosensory pathway in the rat. J Comp Neurol 435:325–340.

Kishimoto T, Sasa M, Takaori S (1991) Inhibition of lateral vestibular nucleus neurons by 5-hydroxytryptamine derived from the dorsal raphe nucleus. Brain Res 553:229–237.

Kosofsky BE, Molliver ME (1987) The serotonergic innervation of cerebral cortex: different classes of axon terminals arise from dorsal and median raphe nuclei. Synapse 1:153–168.

Leger L, Wiklund L (1982) Distribution and numbers of indoleamine cell bodies in the cat brainstem determined with Falck-Hillarp fluorescence histochemistry. Brain Res Bull 9:245–251.

Li JL, Xiong KH, Li YQ, Kaneko T, Mizuno N (2000) Serotonergic innervation of mesencephalic trigeminal nucleus neurons: a light and electron microscopic study in the rat. Neurosci Res 37: 127–140.

Licata F, Li Volsi G, Maugeri G, Santangelo F (1995) Neuronal responses in vestibular nuclei to dorsal raphe electrical stimulation. J Vestib Res 5:137–145.

Liu R, Ding Y, Aghajanian GK (2002a) Neurokinins activate local glutamatergic inputs to serotonergic neurons of the dorsal raphe nucleus. Neuropsychopharmacology 27:329–340.

Liu RJ, van den Pol AN, Aghajanian GK (2002b) Hypocretins (orexins) regulate serotonin neurons in the dorsal raphe nucleus by excitatory direct and inhibitory indirect actions. J Neurosci 22:9453–9464.

Liu R, Jolas T, Aghajanian G (2000) Serotonin 5-HT_2 receptors activate local GABA inhibitory inputs to serotonergic neurons of the dorsal raphe nucleus. Brain Res 873:34–45.

Loewy AD (1981) Raphe pallidus and raphe obscurus projections to the intermediolateral cell column in the rat. Brain Res 222: 129–133.

Ma QP, Yin GF, Ai MK, Han JS (1991) Serotonergic projections from the nucleus raphe dorsalis to the amygdala in the rat. Neurosci Lett 134:21–24.

Marcus DA, Furman JM (2006) Prevention of motion sickness with rizatriptan: a double-blind, placebo-controlled pilot study. Med Sci Monit 12:PI1–PI7.

Marcus DA, Furman JM, Balaban CD (2005) Motion sickness in migraine sufferers. Expert Opin Pharmacother 6:2691–2697.

Marinelli S, Schnell SA, Hack SP, Christie MJ, Wessendorf MW, Vaughan CW (2004) Serotonergic and nonserotonergic dorsal raphe neurons are pharmacologically and electrophysiologically heterogeneous. J Neurophysiol 92:3532–3537.

McLean IW, Nakane PK (1974) Periodate-lysine-paraformaldehyde fixative: a new fixative for immunoelectron microscopy. J Histochem Cytochem 22:1077–1083.

Moore RY (1981) The anatomy of central serotonin systems in the rat brain. In: Serotonin neurotransmission and behavior (Jacobs BL, Gelperin A, eds), pp 35–71. Cambridge, MA: MIT Press.

Moore RY, Halaris AE (1975) Hippocampal innervation by serotonin neurons of the midbrain raphe in the rat. J Comp Neurol 164: 171–184.

Moore RY, Halaris AE, Jones BE (1978) Serotonin neurons of the midbrain raphe: ascending projections. J Comp Neurol 180: 417–438.

Morin LP, Meyer-Bernstein EL (1999) The ascending serotonergic system in the hamster: comparison with projections of the dorsal and median raphe nuclei. Neuroscience 91:81–105.

Nielsen K, Brask D, Knudsen GM, Aznar S (2006) Immunodetection of the serotonin transporter protein is a more valid marker for serotonergic fibers than serotonin. Synapse 59:270–276.

O'Hearn E, Molliver ME (1984) Organization of raphe-cortical projections in rat: a quantitative retrograde study. Brain Res Bull 13: 709–726.

Perna G, Alpini D, Caldirola D, Raponi G, Cesarani A, Bellodi L (2003) Serotonergic modulation of the balance system in panic disorder: an open study. Depress Anxiety 17:101–106.

Petrov T, Krukoff TL, Jhamandas JH (1992) The hypothalamic paraventricular and lateral parabrachial nerve nuclei receive collaterals from raphe nucleus neurons: a combined double retrograde and immunocytochemical study. J Comp Neurol 318:18–26.

Porter JD, Balaban CD (1997) Connections between the vestibular nuclei and brain stem regions that mediate autonomic function in the rat. J Vestib Res 7:63–76.

Ricaurte G, Bryan G, Strauss L, Seiden L, Schuster C (1985) Hallucinogenic amphetamine selectively destroys brain serotonin nerve terminals. Science 229:986–988.

Sakai K, Crochet S (2001) Differentiation of presumed serotonergic dorsal raphe neurons in relation to behavior and wake-sleep states. Neuroscience 104:1141–1155.

Satoh K (1979) The origin of reticulospinal fibers in the rat: a HRP study. J Hirnforsch 20:313–322.

Schmued LC, Hopkins KJ (2000) Fluoro-Jade B: a high affinity fluorescent marker for the localization of neuronal degeneration. Brain Res 874:123–130.

Schuerger RJ, Balaban CD (1999) Organization of the coerulo-vestibular pathway in rats, rabbits, and monkeys. Brain Res Rev 30:189–217.

Serrats J, Mengod G, Cortés R (2005) Expression of serotonin 5-HT_{2C} receptors in GABAergic cells of the anterior raphe nuclei. J Chem Neuroanat 29:83–91.

Sim LJ, Joseph SA (1993) Dorsal raphe nucleus efferents: termination in peptidergic fields. Peptides 14:75–83.

Simon NM, Parker SW, Wernick-Robinson M, Oppenheimer JE, Hoge AE, Worthington JJ, Korbly NB, Pollack MH (2005) Fluoxetine for vestibular dysfunction and anxiety: a prospective pilot study. Psychosomatics 46:334–339.

Simpson KL, Waterhouse BD, Lin RCS (2003) Differential expression of nitric oxide in serotonergic projection neurons: neurochemical identification of dorsal raphe inputs to rodent trigeminal somatosensory targets. J Comp Neurol 466:495–512.

Sotelo C, Cholley B, El Mestikawy S, Gozlan H, Hamon M (1990) Direct immunohistochemical evidence of the existence of 5-HT_{1A} autoreceptors on serotonergic neurons in the midbrain raphe nuclei. Eur J Neurosci 2:1144–1154.

Staab JP, Ruckenstein MJ (2005) Chronic dizziness and anxiety: effect of course of illness on treatment outcome. Arch Otolaryngol Head Neck Surg 131:675–679.

Staab JP, Ruckenstein MJ, Amsterdam JD (2004) A prospective trial of sertraline for chronic subjective dizziness. Laryngoscope 114: 1637–1641.

Staab JP, Ruckenstein MJ, Solomon D, Shepard NT (2002) Serotonin reuptake inhibitors for dizziness with psychiatric symptoms. Arch Otolaryngol Head Surg 128:554–560.

Steinbusch HWM (1981) Distribution of serotonin-immunoreactivity in the central nervous system of the rat: cell bodies and terminals. Neuroscience 6:557–618.

Steinbusch HW, Nieuwenhuys R, Verhofstad AA, Van der Kooy D (1981) The nucleus raphe dorsalis of the rat and its projection upon the caudatoputamen. A combined cytoarchitectonic, immunohistochemical and retrograde transport study. J Physiol (Paris) 77: 157–174.

Switzer RC 3rd (2000) Application of silver degeneration stains for neurotoxicity testing. Toxicol Pathol 28:70–83.

Thompson AM, Thompson GC (2001) Serotonin projection patterns to the cochlear nucleus. Brain Res 907:195–207.

Van Bockstaele EJ, Biswas A, Pickel VM (1993) Topography of serotonin neurons in the dorsal raphe nucleus that send axon collaterals to the rat prefrontal cortex and nucleus accumbens. Brain Res 624:188–198.

Vertes RP (1991) A PHA-L analysis of ascending projections of the dorsal raphe nucleus in the rat. J Comp Neurol 313:643–668.

Vertes RP, Kocsis B (1994) Projections of the dorsal raphe nucleus to the brainstem: PHA-L analysis in the rat. J Comp Neurol 340: 11–26.

Waterhouse BD, Devilbiss D, Seiple S, Markowitz R (2004) Sensorimotor-related discharge of simultaneously recorded, single neurons in the dorsal raphe nucleus of the awake, unrestrained rat. Brain Res 1000:183–191.

Xiong G, Matsushita M (2000) Connections of Purkinje cell axons of lobule X with vestibulocerebellar neurons projecting to lobule X or IX in the rat. Exp Brain Res 133:219–228.

Zhou FC, Azmitia EC (1983) Effects of 5,7-dihydroxytryptamine on HRP retrograde transport from hippocampus to midbrain raphe nuclei in the rat. Brain Res Bull 10:445–451.

Zhou FC, Tao-Cheng JH, Segu L, Patel T, Wang Y (1998) Serotonin transporters are located on the axons beyond the synaptic junctions: anatomical and functional evidence. Brain Res 805: 241–254.

(Accepted 23 March 2007)
(Available online 15 May 2007)